# We are IntechOpen,
# the world's leading publisher of
# Open Access books
# Built by scientists, for scientists

## 4,800
Open access books available

## 122,000
International authors and editors

## 135M
Downloads

Our authors are among the

## 154
Countries delivered to

## TOP 1%
most cited scientists

## 12.2%
Contributors from top 500 universities

CLARIVATE ANALYTICS
BOOK CITATION INDEX
INDEXED

**WEB OF SCIENCE**™

Selection of our books indexed in the Book Citation Index
in Web of Science™ Core Collection (BKCI)

# Interested in publishing with us?
# Contact book.department@intechopen.com

# Nonreciprocal Devices Utilizing Longitudinally Magnetized Ferrite Coupled Lines

Adam Kusiek, Wojciech Marynowski, Rafal Lech and
Jerzy Mazur

Additional information is available at the end of the chapter

### Abstract

This chapter presents authors' recent research on the nonreciprocal devices utilizing longitudinally magnetized ferrite coupled line (FCL) junction. The principle of operation of FCL junction is explained and the hybrid techniques of analysis are shown. Numerical and experimental results concerning the nonreciprocal devices utilizing the different configurations of FCL junctions are presented and discussed.

**Keywords**: ferrite, nonreciprcoal, Faraday rotation

## 1. Introduction

Nonreciprocal devices have been extensively used in modern microwave and millimeter systems [2–4, 14, 25, 27, 28]. In order to obtain the nonreciprocal effects, one needs to utilize the magnetized ferrite materials [2, 4, 14, 25, 27, 28] or active elements such as amplifiers [3]. Recently, the longitudinally magnetized ferrite coupled striplines or slotlines [2, 9, 14, 27] are being developed and employed to realize integrated nonreciprocal devices. Significant interest in these devices results from their advantages which are weak biasing magnetic field and wide operation bandwidth.

The basic part of ferrite coupled line (FCL) devices is longitudinally magnetized FCL section composed of two coupled lines placed on ferrite substrate [6, 21]. This structure was first proposed and experimentally verified by [6]. Next, Next, Mazur & Mrozowski in [21] using the coupled-mode method (CMM) developed the model of FCL section which explains the operation of this structure and gives basis steps in their design procedure. According to this model, in the ferrite section, a gyromagnetic coupling occurs, resulting in Faraday rotation effect. The wide operation bandwidth and high isolation are obtained, when the Faraday

rotation phenomenon is optimal. This optimal effect is achieved when the ferrite material is placed in the region where the wave is linearly polarized and occurs in cylindrical waveguide with coaxially located ferrite rod or suspended stripline. In order to construct devices such as circulators [9, 23], gyrators [19, 22], or isolators [13], the FCL junction has to be cascaded with reciprocal sections providing input signals to the FCL which are either in phase or out of phase [20].

So far, studies concerning FCL devices have been focused mainly on structures realized in a planar line technology [1, 4, 9]. Such structures allow one to obtain fully integrated FCL devices. However, due to the significant length of the ferrite section, the main drawbacks are high insertion losses occurring in ferrite material and large dimensions of the structure.

There were several attempts to improve performance and to reduce total dimensions of planar FCL devices. Promising results concerning low insertion losses and high isolation were obtained for the nonreciprocal devices employing a ferrite coupled slotline [9] and stripline junctions [23, 24]. For the fabricated devices, obtained insertion losses were not lower than 3 dB and isolation was better than 12 dB [9, 18, 23]. Moreover, in order to reduce the dimensions of the planar FCL devices in [4], the circulator with appropriate matching networks at the ports ensuring multiple reflections was proposed. For presented device, the FCL junction length reduction by a factor of two was obtained. The drawback of this structure was high value of insertion losses caused by multiple transmission of signal through the lossy ferrite junction. Also similar length reduction of FCL junction was achieved with the use of periodic left-handed/ferrite coupled line (LH-FCL) structures [1]. However, for the simulated circulator utilizing LH-FCL section, the insertion losses were not lower than 4 dB.

The better performance in comparison to currently proposed planar configurations was obtained for nonreciprocal devices utilizing cylindrical ferrite coupled line (CFCL) junction [10]. Due to the similar geometry to the circular waveguide with coaxially located ferrite rod, such structure allows to obtain close-to-optimal Faraday rotation effect. Moreover, in such configuration, stronger gyromagnetic coupling occurs which is a result of high magnetic field concentration in the ferrite medium. These make possible to design shorter ferrite junctions ensuring lower insertion losses in comparison to planar ones. This junction was successfully applied to realization of nonreciprocal devices such as isolators and circulators [11, 12].

This chapter presents the authors' recent research on the nonreciprocal devices utilizing longitudinally magnetized FCL junction. The operation principle of FCL junction is explained, and the hybrid techniques of analysis are shown. Numerical and experimental results concerning the nonreciprocal devices using different configurations of FCL junctions are presented and discussed.

## 2. Formulation of the problem

The general view of FCL junction is presented in Fig. 1. This junction is a four-port structure that contains a ferrite section realized as two coupled lines placed on ferrite substrate. The ferrite section is fed from dielectric coupled lines with the same cross section where instead of ferrite, the dielectric materials are used. When the ferrite junction is longitudinally magnetized, the Faraday rotation phenomenon occurs, resulting in nonreciprocal properties of the FCL junction. For better understanding of the nonreciprocal effect, an example of a junction ensuring $45°$ Faraday rotation has been considered (see Fig. 1(b) and (c)). When
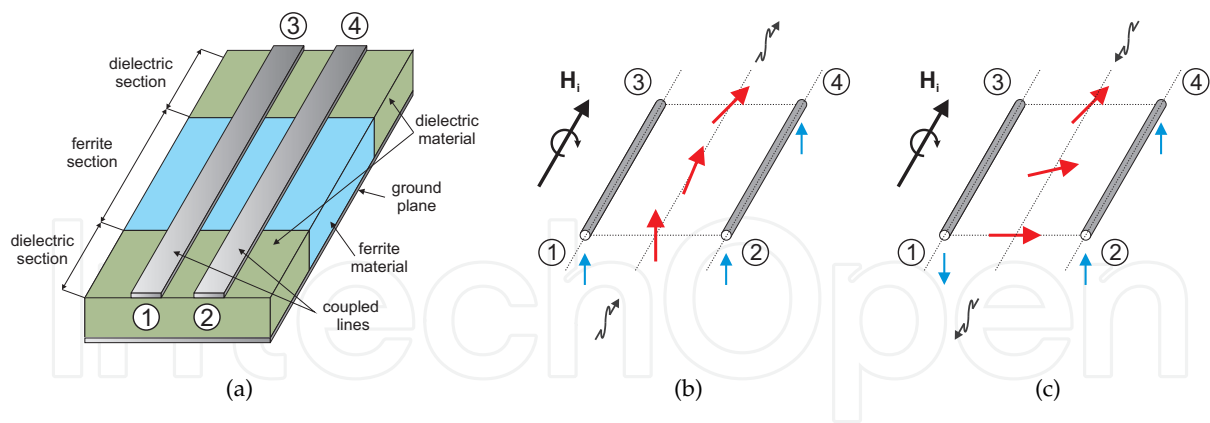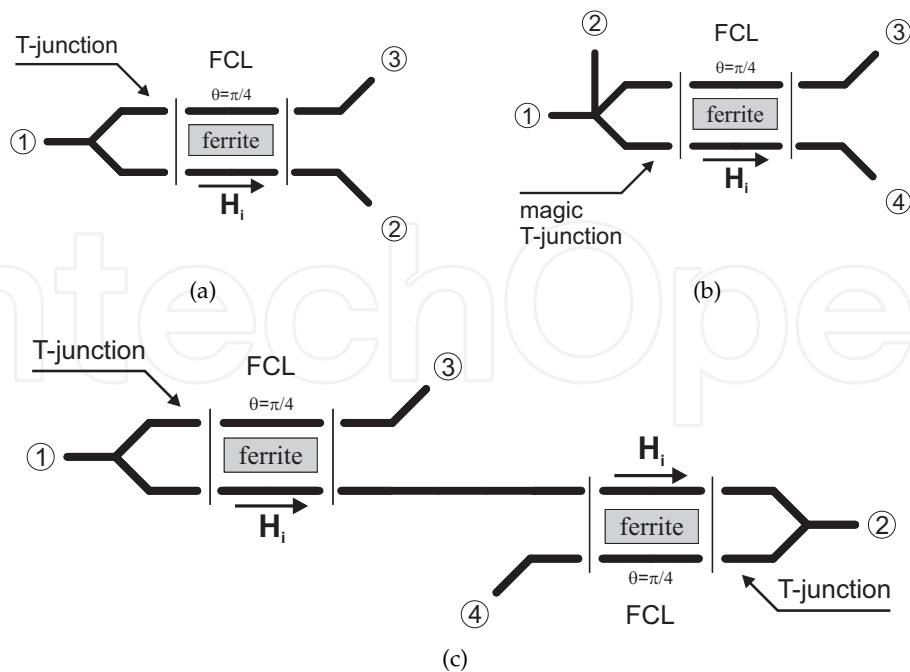
**Figure 1.** Ferrite coupled line junction: (a) general view of the structure and transmission through the junction for (b) even-mode excitation and (c) single-port excitation

ports (1) and (2) of the structure are excited with in phase signals of equal amplitude (see Fig. 1(b)), due to the Faraday rotation, the output signal is observed only at port (4), while port (3) is isolated. On the other hand, when only port (4) of the structure is excited, the out of phase signals of equal amplitudes appear in ports (1) and (2) (see Fig. 1(c)). These phenomena occurring in the FCL section directly indicate the presence of the nonreciprocal effect. Based on the abovementioned phenomena, it was noted in [20] that in order to obtain nonreciprocal transmission, the FCL section should be cascaded with the structures that allow for the even- or odd-mode signal excitation. This makes possible to realize FCL circulators, which can then be used to design a variety of other nonreciprocal circuits such as isolators or phase shifters.

One of the basic nonreciprocal circuits built based on the FCL section is a three-port circulator shown in Fig 2(a). This structure consists of a cascade connection of $T^e$- or $T^o$-junction with four-port FCL junction. Note that the direction of circulation of the circulator structure depends on the choice of T-junction type. Taking into account the circulator with $T^e$-junction, when port (1) of the structure is excited the output signal appears in port (2). Excitation of port (2) of the circulator results in the signal transmission to port (3). Finally, if port (3) is excited, the signal is transmitted to port (1). Therefore, such circuit provides transmission sequence between ports (1) $\rightarrow$ (3) $\rightarrow$ (2) $\rightarrow$ (1). The circulation direction will reverse when the FCL section is cascaded with $T^o$-junction. In addition, the circulation direction can be reversed by changing into opposite the direction of biasing magnetic field which results in reversed direction of Faraday rotation. The described circulator can be used for the realization of isolator, by introducing a matched load in one of the circulator ports.

The four-port circulators can be obtained by replacing in three-port circulator from Fig. 2(a) the normal T-junction with magic T-junction (see Fig. 2(b)) or just by cascading two three-port FCL circulators (see Fig. 2(c)). The advantage of structure from Fig. 2(b) is that the signal for each transmission passes through the ferrite section only once, and as a result, this structure can be characterized by lower insertion losses. However, in the case of integrated circuits, the realization of this circulator requires the design of a complex and technologically demanding magic T-junction. In the case of nonreciprocal devices utilizing two FCL sections, it is possible to obtain better isolation in comparison to structure from Fig. 2(b). However, due to the double signal passing through the ferrite section, the losses of the structure are two times

**Figure 2.** Nonreciprocal devices utilizing ferrite coupled line junction: (a) three-port circulator, (b) four-port circulator with single FCL section, and (c) four-port circulator with double FCL section

higher. It should be noted that presented nonreciprocal devices from Fig. 2 are analogous to cylindrical waveguide nonreciprocal devices with Faraday rotation ([7]).

In order to determine the scattering parameters of the FCL junction, two different hybrid techniques have been proposed and developed ([12, 16–18]) (see Fig. 3). The first approach
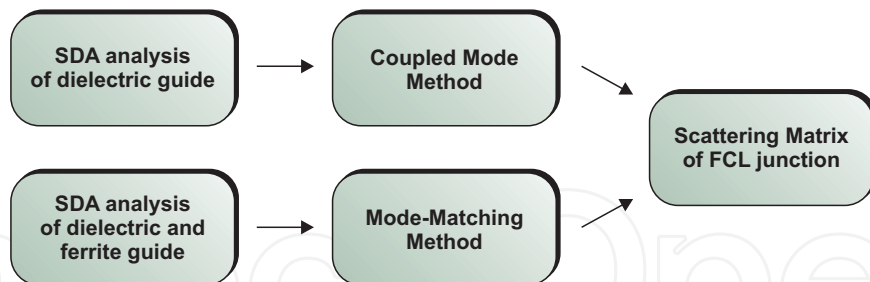


**Figure 3.** Proposed analysis methods of investigated configurations of FCL junctions

is based on the combination of spectral-domain approach (SDA) and coupled-mode method (CMM) ([16, 17]). The analysis using SDA/CMM involves introducing an isotropic basic guide. This guide is complementary to the ferrite one; however, instead of ferrite, the dielectric characterized by the same permittivity as ferrite and relative permeability $\mu_r = 1$ is utilized. In this approach, the basic guide modes obtained from SDA are used to determine the wave parameters of ferrite modes. As a result of the analysis, the dispersion characteristics of the ferrite line, the gyromagnetic coupling coefficient, and the scattering parameters of the ferrite junction are obtained. The second method is based on a combination of SDA with mode-matching (MM) technique ([12, 18]). In this approach, the SDA is utilized to determine the propagation coefficients and field distribution of two fundamental modes in

a dielectric and ferrite section. Then by applying the continuity conditions for the tangential field components at both the interfaces between dielectric and ferrite sections, we formulate the scattering matrix of four-port FCL junction.

The formulation of SDA for dielectric/ferrite guides with different cross sections has been presented in section 2.1. The details of scattering matrix calculation utilizing CMM and MM method have been presented in sections 2.2.1 and 2.2.2, respectively.

## 2.1. Analysis of dielectric/ferrite guide using SDA

In Fig. 4, the cross sections of the investigated lines are presented. In order to determine the propagation coefficients and field distribution in the structure, the spectral domain approach is utilized. Depending on the type of the considered line, the method is formulated in rectangular, cylindrical, or elliptic coordinate system.



(a)                          (b)                          (c)
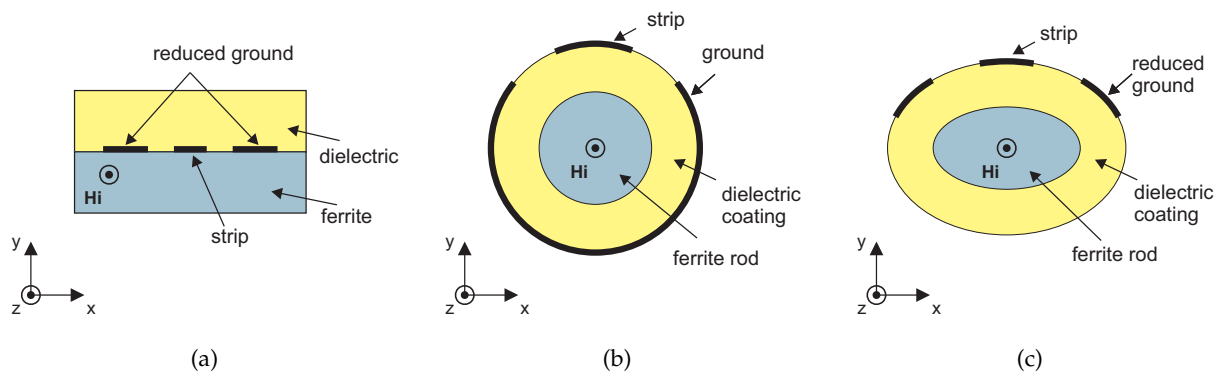
**Figure 4.** Investigated types of coupled lines: (a) planar three-strip line, (b) cylindrical coupled slotline and (c) elliptical three-strip line

The Fourier transform in each coordinate system takes the following form:

- Rectangular coordinates $(x, y, z)$

$$\widetilde{f}(p) = \int_{\mathbb{R}} f(y)e^{-jpy}\,\mathrm{d}y, \quad f(y) = \frac{1}{2\pi}\int_{\mathbb{R}} \widetilde{f}(p)e^{jpy}\,\mathrm{d}p, \tag{1}$$

- Cylindrical coordinates $(\rho, \varphi, z)$

$$\widetilde{f}(p) = \frac{1}{2\pi}\int_{0}^{2\pi} f(\varphi)e^{-jp\varphi}\,\mathrm{d}\varphi, \quad f(\varphi) = \sum_{p=-\infty}^{\infty} \widetilde{f}(p)e^{jp\varphi}, \tag{2}$$

- Elliptic coordinates $(u, v, z)$

$$\widetilde{f}^{e(o)}(p) = \frac{1}{2\pi} \int\limits_0^{2\pi} f(v) \left\{ \begin{array}{c} ce_p(q,v) \\ se_p(q,v) \end{array} \right\} \, dv, \tag{3}$$

$$f(v) = \sum_{p=0}^{\infty} \widetilde{f}^e(p) ce_p(q,v) + \sum_{p=1}^{\infty} \widetilde{f}^o(p) se_p(q,v), \tag{4}$$

where $\widetilde{f}(\cdot)$ is the image of the function $f(\cdot)$, $ce_p(\cdot,\cdot)$ and $se_p(\cdot,\cdot)$ are even and odd angular Mathieu functions of $p$th order, $q = k_0^2 d^2/4$, $k_0 = \omega\sqrt{\mu_0\varepsilon_0}$, and $d$ is the focal length. The electromagnetic field in the structure can be described by Maxwell's equations defined in the spectral domain, as follows:

$$\nabla \times \widetilde{\mathbf{E}} = -k_0 \boldsymbol{\mu}_r \eta \widetilde{\mathbf{H}}, \tag{5}$$

$$\nabla \times \eta \widetilde{\mathbf{H}} = k_0 \varepsilon_r \widetilde{\mathbf{E}}, \tag{6}$$

where $\widetilde{\mathbf{E}}$ and $\widetilde{\mathbf{H}}$ are Fourier transforms of the electric and magnetic fields, respectively, $\eta = -j\eta_0$, $\eta_0 = \sqrt{\mu_0/\varepsilon_0}$, and $\boldsymbol{\mu}_r$ denotes the permeability tensor of ferrite material. For the longitudinally magnetized ferrite material along $z$-axis, $\boldsymbol{\mu}_r = \mathbf{T}\boldsymbol{\mu}_r'\mathbf{T}^{-1}$, where $\boldsymbol{\mu}_r' = \mu(\mathbf{i}_x\mathbf{i}_x + \mathbf{i}_y\mathbf{i}_y) + j\mu_a(\mathbf{i}_x\mathbf{i}_y - \mathbf{i}_y\mathbf{i}_x) + \mathbf{i}_z\mathbf{i}_z$ is a permeability tensor in a dyadic form defined in rectangular coordinates, $\mathbf{T}$ is transformation matrix from rectangular to cylindrical or elliptic coordinates, and $\mu$ and $\mu_a$ are defined according to [7].

By applying the boundary and continuity conditions to the relations (5), (6) and assuming the fields and currents variation along $z$-axis as $e^{-j\beta z}$, one obtains a set of equations combining tangential electric field ($\widetilde{E}_z$ and $\widetilde{E}_\xi$) and current densities ($\widetilde{J}_z$ and $\widetilde{J}_\xi$) at the strips:

$$\begin{bmatrix} \widetilde{E}_z(\varsigma = \varsigma_0, p) \\ \widetilde{E}_\xi(\varsigma = \varsigma_0, p) \end{bmatrix} = [\mathbf{G}(p,\beta)] \begin{bmatrix} \widetilde{J}_\xi(\varsigma = \varsigma_0, p) \\ \widetilde{J}_z(\varsigma = \varsigma_0, p) \end{bmatrix}, \tag{7}$$

where $(\varsigma,\xi) = \{(x,y),(\rho,\varphi),(u,v)\}$ and $\mathbf{G}(p,\beta)$ is a dyadic Green's function ([8]). In order to solve (7) the current on the patch is expanded in terms of basis functions:

$$J_\xi(\xi) = \begin{cases} \sum\limits_{n=1}^{N} a_n \sin\left(\frac{n\pi(2\xi+w)}{2w}\right), & |\xi| \leq \frac{w}{2} \\ \\ 0, & \text{otherwise}, \end{cases} \tag{8}$$

$$J_z(\xi) = \begin{cases} \sum\limits_{n=0}^{N} b_n \dfrac{\cos\left(\frac{n\pi(2\xi+w)}{2w}\right)}{\sqrt{1-\left(\frac{2\xi}{w}\right)^2}}, & |\xi| \leq \frac{w}{2} \\ \\ 0, & \text{otherwise}, \end{cases} \tag{9}$$

where $a_n$ and $b_n$ are unknown current expansion coefficients. Next, using MoM with current basis functions (8) and (9) chosen as a testing functions (Galerkin method) a homogeneous set of equations is obtained ([26]). The nontrival solutions of the problem provide us with a phase coefficients $\beta$ and corresponding current coefficients allowing us to determine the current density distributions on the strips as well as the electric and magnetic fields in the cross section of the structure.

## 2.2. Scattering matrix of ferrite coupled junction

### 2.2.1. Coupled-mode method

Using the coupled-mode method, a gyromagnetic coupling coefficient, propagation coefficients of ferrite modes, and scattering matrix of FCL junction can be determined ([5, 21]). In this method, the transverse electric and magnetic fields in the investigated ferrite guide are expressed in terms of basic guide field eigenfunctions. Assuming two fundamental modes propagated in the basic guide, the Maxwell's equations for basic and ferrite guides are combined together, and after some mathematical manipulation, the following set of coupled-mode equations is obtained:

$$
\begin{aligned}
\frac{\partial}{\partial z}\widehat{U}_e(z) + \mathrm{j}\beta_e Z_e \widehat{I}_e(z) &= C_{eo}\widehat{I}_o(z), \\
\frac{\partial}{\partial z}\widehat{U}_o(z) + \mathrm{j}\beta_o Z_o \widehat{I}_o(z) &= C_{oe}\widehat{I}_e(z), \\
\frac{\partial}{\partial z}\widehat{I}_e(z) + \mathrm{j}\beta_e Y_e \widehat{U}_e(z) &= 0, \\
\frac{\partial}{\partial z}\widehat{I}_o(z) + \mathrm{j}\beta_o Y_o \widehat{U}_o(z) &= 0,
\end{aligned}
\tag{10}
$$

where

$$
C_{eo} = -C_{eo}^* = k_0 \eta_0 \mu_a \int_{\Omega_f} \left( \mathbf{h}_{t,e} \times \mathbf{h}_{t,o}^* \right) \cdot \mathbf{i}_z \, \mathrm{d}\Omega_f
\tag{11}
$$

define the coupling between two fundamental modes in the basic guide, $\widehat{U}_{e(o)}(z)$ and $\widehat{I}_{e(o)}(z)$ are $z$-dependent voltage and current functions in the ferrite guide, $Z_{e(o)} = 1/Y_{e(o)}$ are wave impedances of fundamental modes, $\mathbf{h}_{t,e(o)}$ are the eigenfunctions of magnetic fields of fundamental modes, and $\Omega_f$ is a ferrite area in the cross section. Next, taking into consideration field distributions $\mathbf{H}_{t,e(o)}$ of basic modes instead of their eigenfunction $\mathbf{h}_{t,e(o)}$, the gyromagnetic coupling coefficient can be written as follows:

$$
C_{eo} = k_0 \eta_0 \mu_a \frac{\sqrt{Z_e Z_o}}{\sqrt{P_e P_o}} \int_{\Omega_f} \left( \mathbf{H}_{t,e} \times \mathbf{H}_{t,o}^* \right) \cdot \mathbf{i}_z \, \mathrm{d}\Omega_f,
\tag{12}
$$

where $P_{e(o)}$ denotes powers of two fundamental basis modes. As one can see, the gyromagnetic coupling occurs in the guide when the ferrite is placed in the area where

magnetic field vectors of two fundamental modes are orthogonal to each other and linearly polarized.

The above-defined transmission line model of the ferrite guide can be used to determine scattering matrix of FCL junction. At first, utilizing symmetry properties of the investigated structure, the modal even/odd voltage and current can be related to voltage and current defined for each of two coupled lines (see Fig. 5)
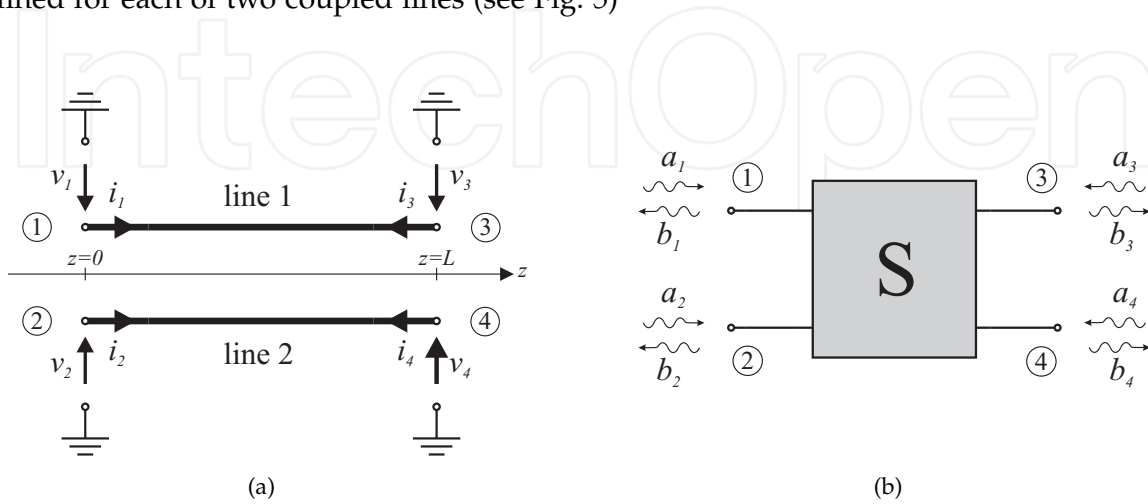


**Figure 5.** Four-port FCL junction: (a) circuit model, (b) network representation

as follows:

$$
\begin{aligned}
\widehat{U}_e(z) &= \widehat{U}_1(z) + \widehat{U}_2(z), & \widehat{I}_e(z) &= \widehat{I}_1(z) + \widehat{I}_2(z), \\
\widehat{U}_o(z) &= \widehat{U}_1(z) - \widehat{U}_2(z), & \widehat{I}_o(z) &= \widehat{I}_1(z) - \widehat{I}_2(z).
\end{aligned}
\tag{13}
$$

Next, applying the above relations to (10), the following eigenproblem is obtained:

$$
\mathbf{QK} = \mathbf{Kk},
\tag{14}
$$

where matrix $\mathbf{Q}$, diagonal matrix of eigenvalues $\mathbf{k}$, and matrix of eigenvectors $\mathbf{K}$ are defined in [10]. The solutions of (14) are the eigenvalues $k_1$ and $k_2$, defining propagation coefficients of two fundamental modes in ferrite guide which take the following form:

$$
k_{1,2} = \pm\sqrt{\frac{\beta_e^2 + \beta_o^2}{2} \pm \sqrt{\left(\frac{\beta_e^2 - \beta_o^2}{2}\right)^2 + \frac{C_{eo}^2}{Z_e Z_o}\beta_e\beta_o}}.
\tag{15}
$$

As one can see, the increase of the coupling results in the increase of the difference between $k_1$ and $k_2$. Finally, the length of the ferrite section ensuring $45^\circ$ Faraday rotation decreases when the coupling $C_{eo}$ increases.

Using the solution of (15), the voltage and current in each of the two coupled lines can be defined at considered $z$ cross section as follows:

$$\begin{bmatrix} \widehat{U}_1(z) \\ \widehat{U}_2(z) \\ \widehat{I}_1(z) \\ \widehat{I}_2(z) \end{bmatrix} = \mathbf{K} \begin{bmatrix} e^{-jk_1z} & 0 & 0 & 0 \\ 0 & e^{jk_1z} & 0 & 0 \\ 0 & 0 & e^{-jk_2z} & 0 \\ 0 & 0 & 0 & e^{jk_2z} \end{bmatrix} \begin{bmatrix} A_1^+ \\ A_1^- \\ A_2^+ \\ A_2^- \end{bmatrix}, \tag{16}$$

where $A_1^{+(-)}$ and $A_2^{+(-)}$ are unknown amplitudes of the forward and backward partial waves in the equivalent transmission line. Assuming notation from Fig. 5(a) and utilizing (16), we can write the relations between voltages and currents in the ports of the considered junction defined at interfaces $z = 0$ and $z = L$:

$$\begin{bmatrix} \widehat{U}_1(z) \\ \widehat{U}_2(z) \\ \widehat{I}_1(z) \\ \widehat{I}_2(z) \end{bmatrix}_{z=0} = \begin{bmatrix} v_1 \\ v_2 \\ i_1 \\ i_2 \end{bmatrix} \quad \text{and} \quad \begin{bmatrix} \widehat{U}_1(z) \\ \widehat{U}_2(z) \\ \widehat{I}_1(z) \\ \widehat{I}_2(z) \end{bmatrix}_{z=L} = \begin{bmatrix} v_3 \\ v_4 \\ -i_3 \\ -i_4 \end{bmatrix}. \tag{17}$$

Combining equations (16) and (17), we obtain the following relation:

$$\begin{bmatrix} v_3 \\ v_4 \\ -i_3 \\ -i_4 \end{bmatrix} = \mathbf{K} \begin{bmatrix} e^{-jk_1L} & 0 & 0 & 0 \\ 0 & e^{jk_1L} & 0 & 0 \\ 0 & 0 & e^{-jk_2L} & 0 \\ 0 & 0 & 0 & e^{jk_2L} \end{bmatrix} \mathbf{K}^{-1} \begin{bmatrix} v_1 \\ v_2 \\ i_1 \\ i_2 \end{bmatrix}. \tag{18}$$

Finally, we define incident and reflected waves in each $i$th port of the structure as follows:

$$a_i = \frac{v_i}{\sqrt{Z_0}} + i_i \sqrt{Z_0} \quad \text{and} \quad b_i = \frac{v_i}{\sqrt{Z_0}} - i_i \sqrt{Z_0},$$

where $Z_0$ is a wave impedance of the port. Applying above relations to (18), we obtain the scattering matrix of four-port FCL junction which is defined as follows:

$$\begin{bmatrix} b_1 \\ b_2 \\ b_3 \\ b_4 \end{bmatrix} = \begin{bmatrix} S_{11} & S_{12} & S_{13} & S_{14} \\ S_{21} & S_{22} & S_{23} & S_{24} \\ S_{31} & S_{32} & S_{33} & S_{34} \\ S_{41} & S_{42} & S_{43} & S_{44} \end{bmatrix} \begin{bmatrix} a_1 \\ a_2 \\ a_3 \\ a_4 \end{bmatrix}. \tag{19}$$

Assuming instead of the voltage and current waves the real voltage and current distribution in the proposed transmission line model of FCL junction, the wave impedances $Z_{e(o)}$ and $Z_0$ can be treated as characteristic impedances.

### 2.2.2. Mode-matching method

In order to determine the S-matrix of the proposed FCL junction, the mode-matching method is utilized. At first, the junction is analyzed as a two-port structure composed of dielectric section followed by ferrite section and another dielectric section as presented in Fig. 6. Since
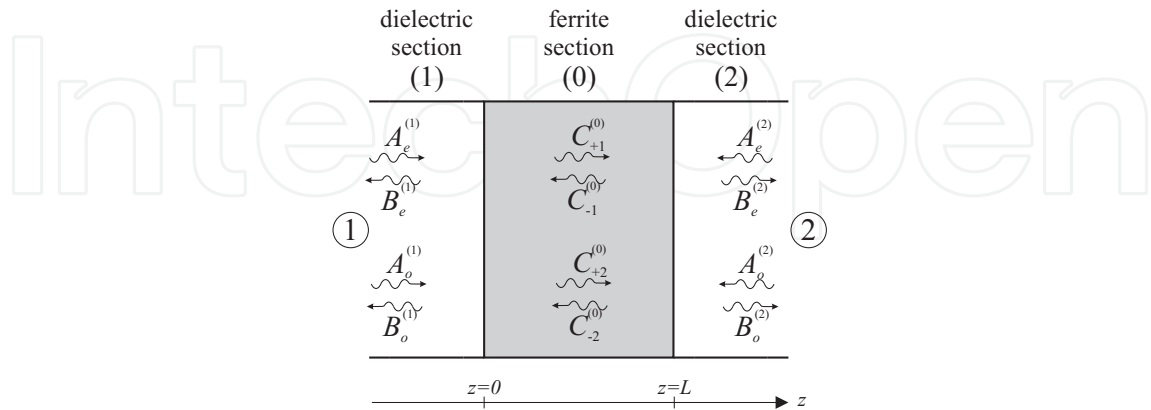


**Figure 6.** Two port FCL junction composed of ferrite and dielectric sections.

the widths of the strips in the ferrite and dielectric sections are the same, the higher modes are not excited, and therefore, they are neglected in the analysis. In this case, only two fundamental modes are taken into consideration. The modes propagated in the dielectric and ferrite sections are called dielectric and ferrite waves, respectively. Due to the symmetry of the structure, we can distinguish even- and odd-mode waves in the dielectric section. Despite the fact that at port (1) or (2) only one of the dielectric waves can appear, both ferrite waves are excited. The wave parameters and field distributions of modes in the ferrite and dielectric sections are determined using SDA ([15]). The total field in each section is determined as a superposition of both modes propagating in forward $(+)$ and backward $(-)$ directions. Using the notation from Fig. 6, the total field in dielectric sections $i = 1, 2$ can be written in the following form:

$$\mathbf{F}_t^{(i)} = \left[\mathbf{F}_{+e}^{(i)}, \mathbf{F}_{+o}^{(i)}, \mathbf{F}_{-e}^{(i)}, \mathbf{F}_{-o}^{(i)}\right] \begin{bmatrix} A_e^{(i)} \\ A_o^{(i)} \\ B_e^{(i)} \\ B_o^{(i)} \end{bmatrix}, \tag{20}$$

where $\mathbf{F} = (\mathbf{E}, \mathbf{H})$ represents tangential electric or magnetic field and $A$ and $B$ are the unknown expansion coefficients describing forward and backward waves, respectively, of even $(e)$ and odd $(o)$ modes. The total field in ferrite section can be written as follows:

$$\mathbf{F}_t^{(0)} = \left[\mathbf{F}_{+1}^{(0)}, \mathbf{F}_{+2}^{(0)}, \mathbf{F}_{-1}^{(0)}, \mathbf{F}_{-2}^{(0)}\right] \mathbf{D}(z) \begin{bmatrix} C_{+1}^{(0)} \\ C_{+2}^{(0)} \\ C_{-1}^{(0)} \\ C_{-2}^{(0)} \end{bmatrix}, \tag{21}$$

where $\mathbf{D}(z) = \mathrm{diag}([e^{jk_{+1}^{(0)}z}, e^{jk_{+2}^{(0)}z}, e^{jk_{-1}^{(0)}z}, e^{jk_{-2}^{(0)}z}])$, $k_{\pm1(2)}^{(0)}$ are the propagation coefficients of both fundamental modes in ferrite section and $\mathbf{F} = (\mathbf{E}, \mathbf{H})$ and $C_{\pm1(2)}^{(0)}$ are the unknown expansion coefficients describing forward $(+)$ and backward $(-)$ waves. Using relations (20) and (21), the continuity conditions for the tangential components of electric and magnetic fields at two interfaces $z = 0$ and $z = L$ can be written as follows:

$$\mathbf{E}_t^{(1)}\big|_{z=0} = \mathbf{E}_t^{(0)}\big|_{z=0'}, \qquad \mathbf{H}_t^{(1)}\big|_{z=0} = \mathbf{H}_t^{(0)}\big|_{z=0'} \qquad (22)$$

$$\mathbf{E}_t^{(2)}\big|_{z=L} = \mathbf{E}_t^{(0)}\big|_{z=L'}, \qquad \mathbf{H}_t^{(2)}\big|_{z=L} = \mathbf{H}_t^{(0)}\big|_{z=L}. \qquad (23)$$

This set of equations can be solved using the orthogonality expansion method. As a result, the relation between forward and backward waves in dielectric sections can be derived in the following form:

$$\mathbf{B}' = \mathbf{S}'\mathbf{A}', \qquad (24)$$

where

$$\mathbf{S}' = \begin{bmatrix} S_{ee}^{11} & S_{eo}^{11} & S_{ee}^{12} & S_{eo}^{12} \\ S_{oe}^{11} & S_{oo}^{11} & S_{oe}^{12} & S_{oo}^{12} \\ S_{ee}^{21} & S_{eo}^{21} & S_{ee}^{22} & S_{eo}^{22} \\ S_{oe}^{21} & S_{oo}^{21} & S_{oe}^{22} & S_{oo}^{22} \end{bmatrix}. \qquad (25)$$

and $\mathbf{A}'$ and $\mathbf{B}'$ are the vectors of unknown expansion coefficients for the fields in each section $\mathbf{A}' = [A_e^{(1)}, A_o^{(1)}, A_e^{(2)}, A_o^{(2)}]^T$, $\mathbf{B}' = [B_e^{(1)}, B_o^{(1)}, B_e^{(2)}, B_o^{(2)}]^T$. The $\mathbf{S}'$ matrix defines the two-mode scattering matrix of two-port FCL junction. The element $S_{nm}^{ji}$ defines the relation between $m$ incident wave in the $i$th port and $n$ reflected wave in the $j$th port, where $m, n = \{e, o\}$ and $i, j = \{1, 2\}$.

In the designing procedure of the integrated nonreciprocal devices, more useful is the S-matrix defined from the point of view of the incident and reflected waves at four ports of the FCL junction. The scheme of such junction is presented in Fig. 7.
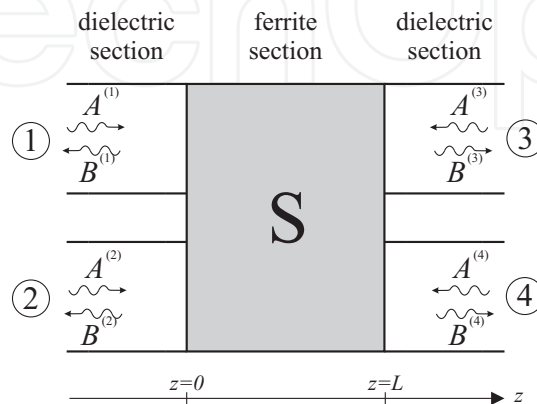


**Figure 7.** Four-port FCL junction

Using the symmetry properties of the even and odd modes propagated in the dielectric sections, the matrix $\mathbf{S}'$ can be rearranged in terms of port waves, and finally, the scattering matrix of four-port FCL junction is obtained. The incident and reflected waves at $i$th port are denoted by $A^{(i)}$ and $B^{(i)}$, respectively. Due to symmetry of the waves in the dielectric sections, they can be written as superpositions of waves in each port of four-port FCL junction as follows:

$$
\begin{aligned}
A_e^{(1)} &= (A^{(1)} + A^{(2)})/\sqrt{2}, & A_o^{(1)} &= (A^{(1)} - A^{(2)})/\sqrt{2}, \\
B_e^{(1)} &= (B^{(1)} + B^{(2)})/\sqrt{2}, & B_o^{(1)} &= (B^{(1)} - B^{(2)})/\sqrt{2}, \\
A_e^{(2)} &= (A^{(3)} + A^{(4)})/\sqrt{2}, & A_o^{(2)} &= (A^{(3)} - A^{(4)})/\sqrt{2}, \\
B_e^{(2)} &= (B^{(3)} + B^{(4)})/\sqrt{2}, & B_o^{(2)} &= (B^{(3)} - B^{(4)})/\sqrt{2}.
\end{aligned}
\tag{26}
$$

which can be expressed in the matrix form

$$
\mathbf{A}' = \mathbf{T}\mathbf{A} \qquad \text{and} \qquad \mathbf{B}' = \mathbf{T}\mathbf{B},
\tag{27}
$$

where $\mathbf{A} = [A^{(1)}, A^{(2)}, A^{(3)}, A^{(4)}]^T$, $\mathbf{B} = [B^{(1)}, B^{(2)}, B^{(3)}, B^{(4)}]^T$, and

$$
\mathbf{T} = \begin{bmatrix} \mathbf{T}_1 & \mathbf{0} \\ \mathbf{0} & \mathbf{T}_1 \end{bmatrix}, \quad \mathbf{T}_1 = \frac{1}{\sqrt{2}} \begin{bmatrix} 1 & 1 \\ 1 & -1 \end{bmatrix}.
$$

Finally, using the two-mode S-matrix (24) and relations (27), the scattering matrix of the four-port FCL junction is obtained.

$$
\mathbf{B} = \mathbf{S}\,\mathbf{A}, \qquad \text{where} \qquad \mathbf{S} = \mathbf{T}^{-1}\,\mathbf{S}'\,\mathbf{T}.
\tag{28}
$$

Such S-matrix can be used in the analysis of the transmission properties of FCL junction with the assumed excitation.

## 3. Numerical results

### 3.1. Microstrip ferrite coupled line junction

The first investigated structure is a planar microstrip ferrite coupled line (MFCL) junction presented in Fig. 8(a). The cross section of the junction is shown in Fig. 8(b). It is a multilayer structure in which two conductive strips are placed at $h_2$ interface while the ground is placed at $h_1$ interface. A ferrite material with a relative permittivity $\varepsilon_{r2} = 13.3$, saturation magnetization $M_s = 239$ kA/m, internal bias $H_i = 0$, and thickness $d_2 = 0.5$ mm is placed in layer (2) located above the conductive strips. The dielectric sections have the same cross section as ferrite section, although instead of ferrite, a dielectric material is used with relative permeability $u_r = 1$ and with the same relative permittivity as the ferrite material. The investigated structure has a plane of symmetry $AA'$ passing through the center of the gap
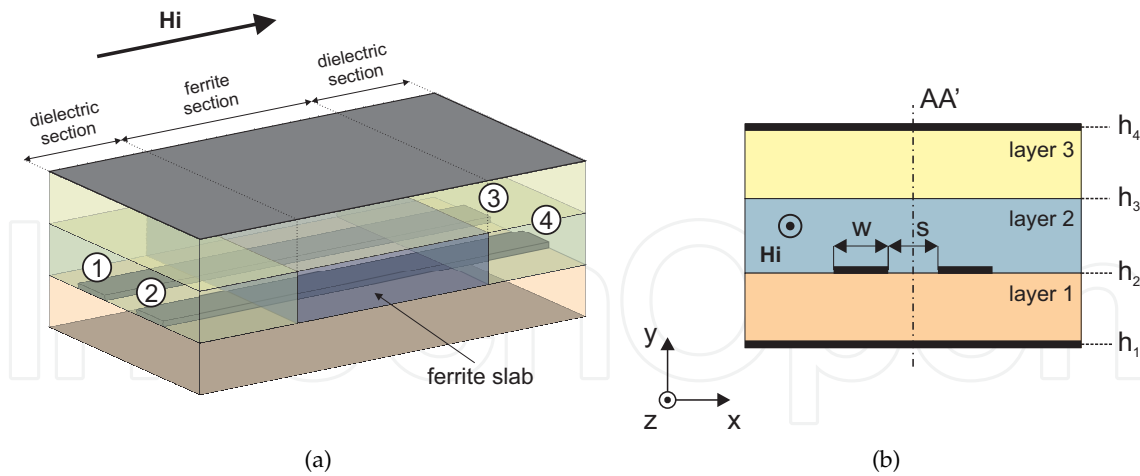
**Figure 8.** Planar junction of microstrip ferrite coupled lines: (a) 3D view and (b) cross section of ferrite guide

between the strips. In the dielectric section, this symmetry plane is an electric or magnetic wall for odd or even mode, respectively.

Utilizing the developed method of analysis, described in section 2, the dispersion characteristics of the investigated structure are first calculated. The calculations were performed in the frequency range from 9 to 18 GHz. The characteristics of the propagation coefficients of the two basic modes propagating in dielectric and ferrite sections are shown in Fig. 9(a). The ferrite modes have a cutoff frequency near $f_M = \gamma(H_i + M_s) = 8.4$ GHz where gyromagnetic coefficient $\gamma = 35.2$ MHz m/kA. This means that the ferrite modes propagate in this structure, when the $\mu_{eff} = (\mu^2 - \mu_a^2)/\mu > 0$, where $\mu$ and $\mu_a$ are the elements of relative permeability tensor defined in section 2.1. It can be noted that with the increasing frequency, the propagation coefficients of the modes in the ferrite line converge to propagation coefficients of the modes in dielectric line. This effect is due to the fact that with
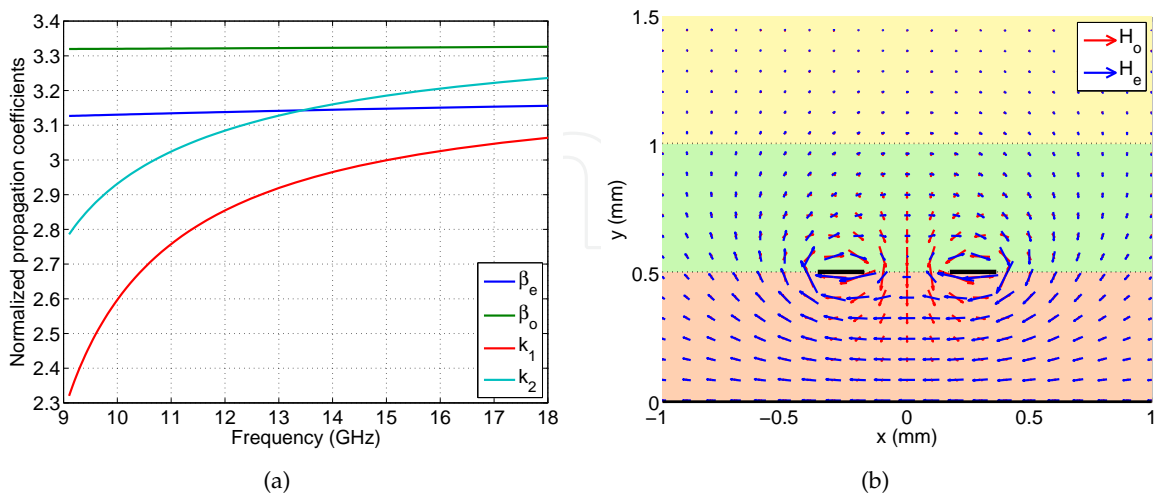


**Figure 9.** Simulation results of MFCL junction: (a) dispersion characteristics and (b) magnetic field distribution of even and odd mode in dielectric section of MFCL junction at $f_0 = 12.4$ GHz

the increase of frequency, the value of $\mu_a$ element of the permeability tensor (responsible for gyromagnetic property of the ferrite) decreases.

Figure 9(b) shows the distributions of the transverse components of magnetic fields for the even and odd modes in the dielectric section. Calculations are performed at frequency $f_0 = 12.4$ GHz. As can be seen, the magnetic field vectors of the dielectric modes are orthogonal to each other in the areas above and below the strips in the symmetry plane $AA'$ of the structure. According to the definition of coupling coefficient (12), if instead of one of these layers the ferrite material is introduced, the optimal gyrotropic coupling effect will be obtained.

In the next step, utilizing the MM method described in section 2.2.2, the scattering parameters of the investigated MFCL junction are determined. The scattering parameters of the junction in a function of ferrite section length at $f_0 = 12.4$ GHz are shown in Fig. 10. The optimal
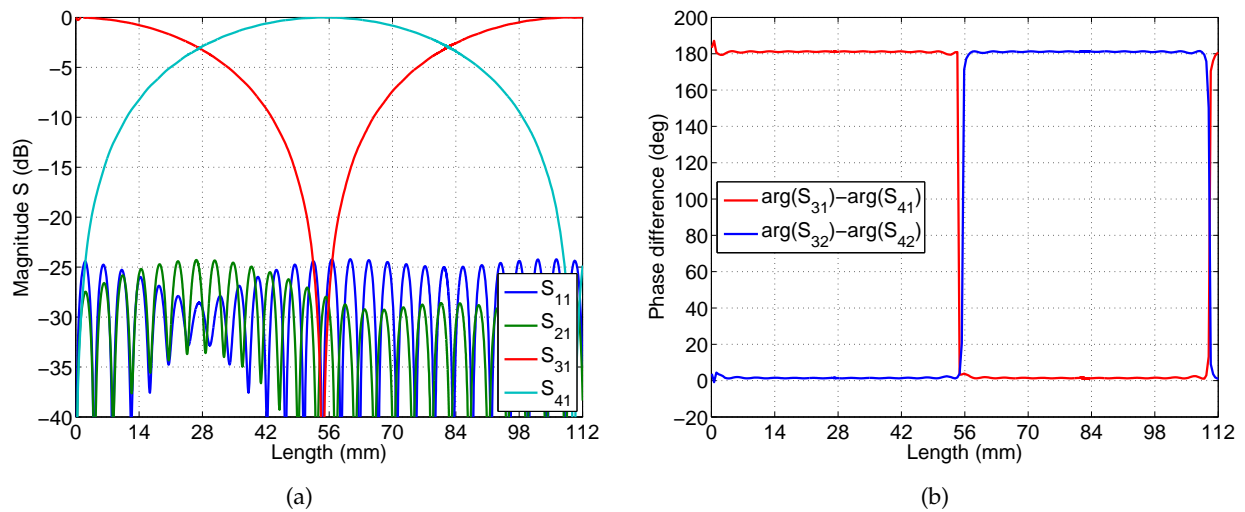


**Figure 10.** Simulated scattering parameters of MFCL junction versus length of ferrite section at $f_0 = 12.4$ GHz: (a) magnitude and (b) phase difference

length $L$ of the ferrite section providing $45°$ Faraday rotation is determined by amplitude and phase conditions ([21]). According to these conditions, when port (1) of the structure is excited, the signal should be equally divided between ports (3) and (4) of the structure, while port (2) should be isolated. Moreover, the phase difference between signals in ports (3) and (4) for ports (1) or (2) excitation should be equal to 0 or $\pm180°$. From the obtained results, it can be seen that optimal length of the section for which the amplitude and phase conditions are fulfilled is $L = 28$ mm.

In order to illustrate the nonreciprocal properties occurring in the investigated FCL, the change of power concentration along the structure has been calculated and presented in Fig. 11.

Based on the obtained results, one can see the periodic effect of signal exchange between coupled lines in the ferrite section due to the Faraday rotation phenomenon. Furthermore, the distributions of the electric and magnetic fields in the input and output ports of FCL junction providing $45°$ Faraday rotation angle ($L = 28$ mm) have been calculated and
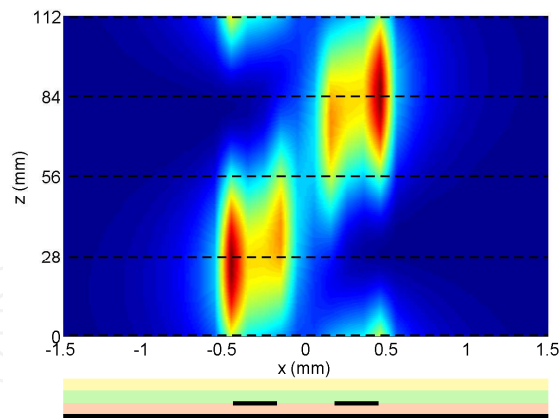
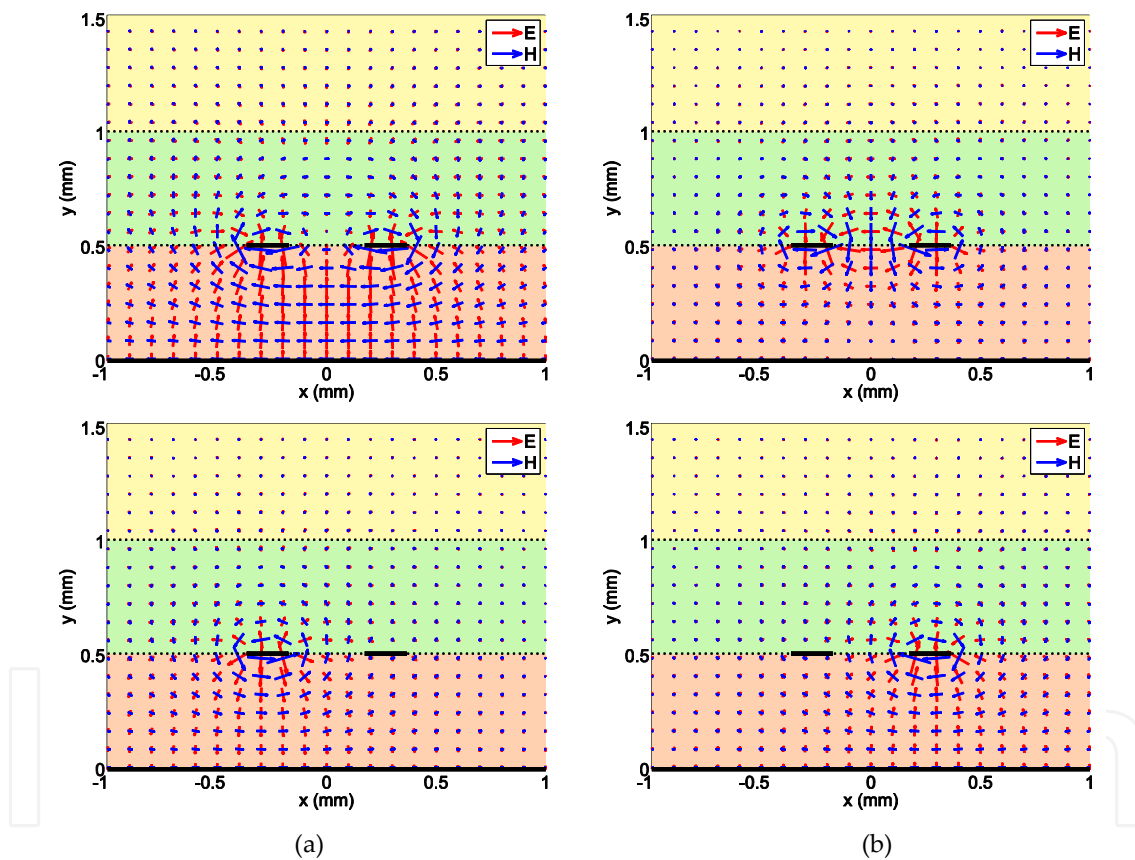**Figure 11.** Power density distribution along the investigated MFCL section



**Figure 12.** Field distribution in dielectric section of MFCL junction at $z = 0$ (upper row) and $z = 28$ mm (bottom row) mm for: (a) even-mode excitation and (b) odd-mode excitation

presented in Fig. 12. In the analysis, the even- and odd-mode excitations of the junction were assumed. From the presented results, it can be observed that when such junction is excited with the even or odd mode, the signal concentrates around the left or right line at the output of the structure. If the direction of the magnetization will be reversed, the signal will concentrate on the opposite strips.

For the FCL junction with the optimal length $L = 28$ mm of the ferrite section, the scattering parameters were calculated in a function of frequency (see Fig. 13).
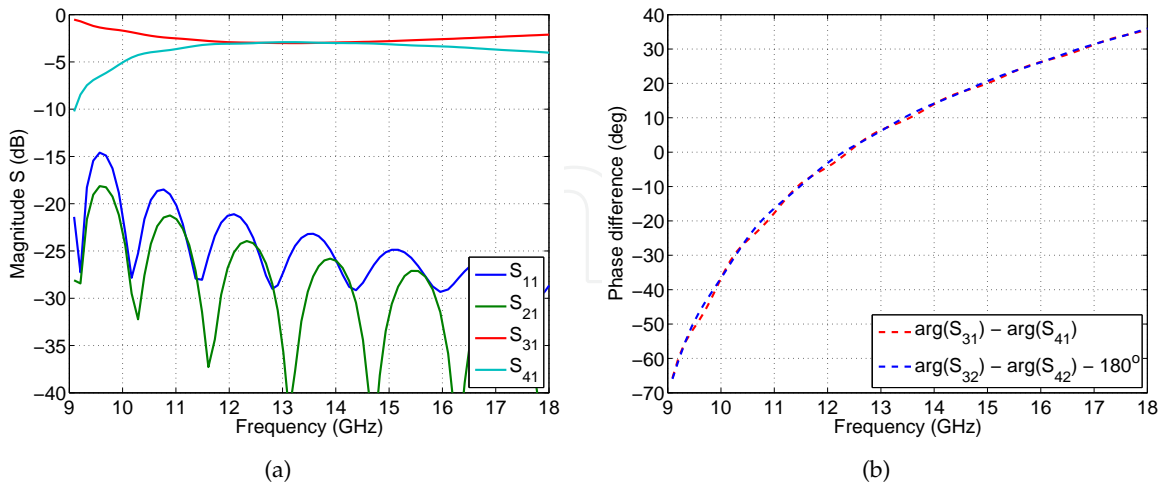


**Figure 13.** Simulated frequency-dependent scattering parameters of MFCL junction: (a) magnitude and (b) phase difference

From the obtained results, it can be seen that the transmission coefficients $S_{31}$ and $S_{41}$ are equal to $-3 \pm 0.5$ dB in the frequency range from 11 to 16 GHz, with isolation $S_{21}$ and reflection losses $S_{11}$ better than $-20$ dB. In the considered frequency range, the phase difference between the output signals in ports (3) and (4) for ports (1) or (2) excitation varies in the range from $-18$ to $27\,^{\circ}$ (see Fig. 13(b)). The optimal $45\,^{\circ}$ Faraday rotation angle is obtained for $f_0 = 12.4$ GHz.

## 3.2. Cylindrical ferrite coupled line junction

Another investigated structure is a cylindrical ferrite coupled line (CFCL) junction. The cross section of ferrite coupled lines is shown in Fig. 14.
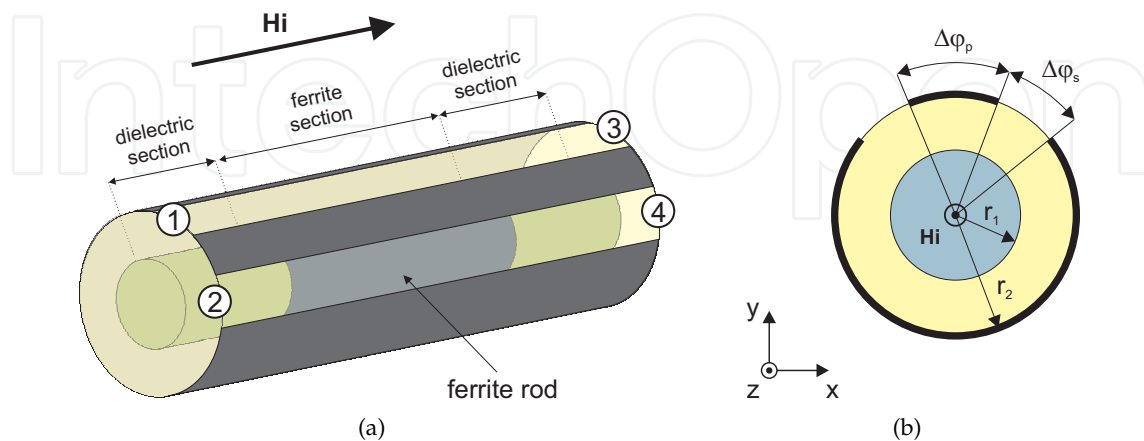


**Figure 14.** Cylindrical ferrite coupled line junction: (a) 3D view and (b) cross section of ferrite guide

This structure consists of a cylindrical ferrite rod of radius $r_1$ covered with dielectric layer of thickness $d = r_2 - r_1$ on which the conductive strips are etched. The dielectric section has the same cross section as ferrite section; however, instead of a ferrite rod, a dielectric rod is used with relative permeability $\mu_r = 1$ and the same relative permittivity as the ferrite material.

Utilizing the developed method of analysis, described in section 2.1, the dispersion characteristics of the investigated structure are first calculated. In the analysis, the following dimensions and material parameters of the junction were assumed: $r_1 = 2.2$ mm, $\varepsilon_{rf} = 15$, saturation magnetization $M_s = 131$ kA/m, internal bias $H_i = 0$, and dielectric coating: $d = 0.127$ mm, $\varepsilon_{rd} = 2.2$. The angular slot/strip widths were $\Delta\varphi_p = 25°$, $\Delta\varphi_s = 15°$. The characteristics of the propagation coefficients of the dielectric and the ferrite lines are shown in Fig. 15(a).
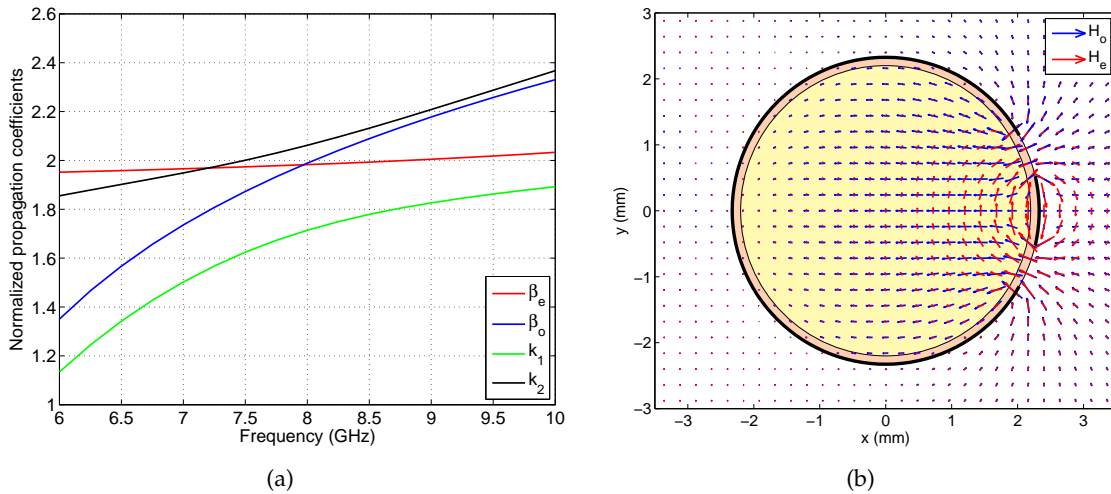


**Figure 15.** Simulation results of CFCL junction: (a) dispersion characteristics and (b) magnetic field distributions of even and odd modes in dielectric section of CFCL junction at $f_0 = 8.2$ GHz

Based on the obtained characteristics for the investigated dielectric lines, it can be noted that for a specific frequency $f_0 = 8$ GHz, the phase velocities of the even and odd modes are equal. It means that in such a line, the isotropic coupling vanishes and only gyromagnetic coupling occurs. This allows to obtain the optimal conditions for the Faraday rotation.

Figure 15(b) shows the magnetic field distributions of the even and odd modes in dielectric line specified for $f_0 = 8.2$ GHz. From these distributions, it can be seen that there are areas in the line where the magnetic fields of both modes are orthogonal; hence, placing the ferrite material in this area of a line will produce the gyromagnetic coupling between the basic field modes.

In the next step, the scattering parameters of CFCL junction are calculated in a function of ferrite section length at $f_0 = 8.2$ GHz and shown in Fig 16.

From the presented results, it can be noticed that the optimal length of the ferrite section providing $45°$ Faraday rotation is $L = 26$ mm. For such length of section $S_{31} = S_{41} = -3$ dB and the phase difference between signals in ports (3) and (4) for ports (1) and (2), excitation is then 0 or $\pm180°$.

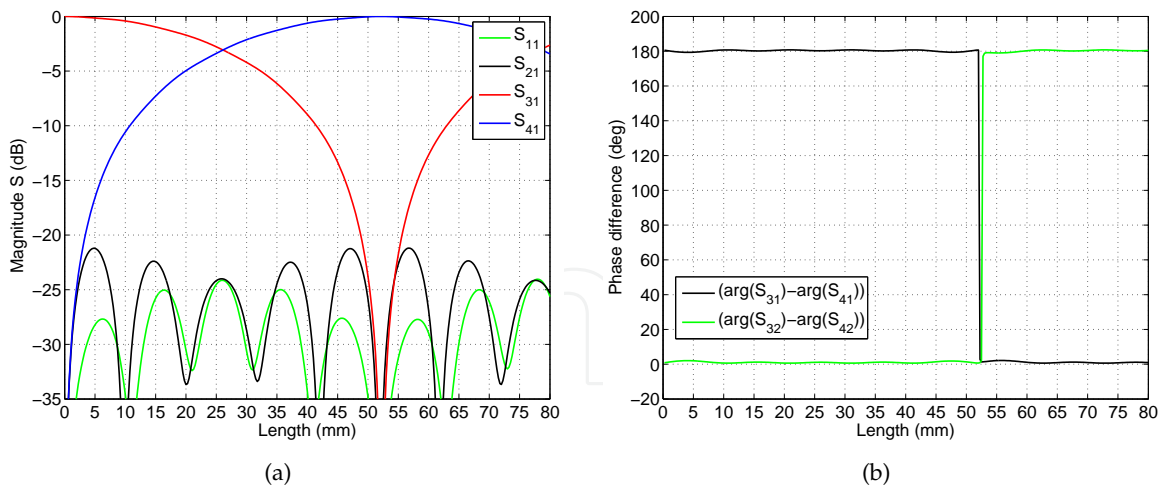(a)                                                            (b)

**Figure 16.** Scattering parameters of CFCL junction versus length of ferrite section: (a) magnitude and (b) phase difference

Similarly to the planar case presented in section 3.1, in order to illustrate the nonreciprocal properties occurring in the investigated CFCL junction, the power concentration along the structure has been determined (see Fig. 17).
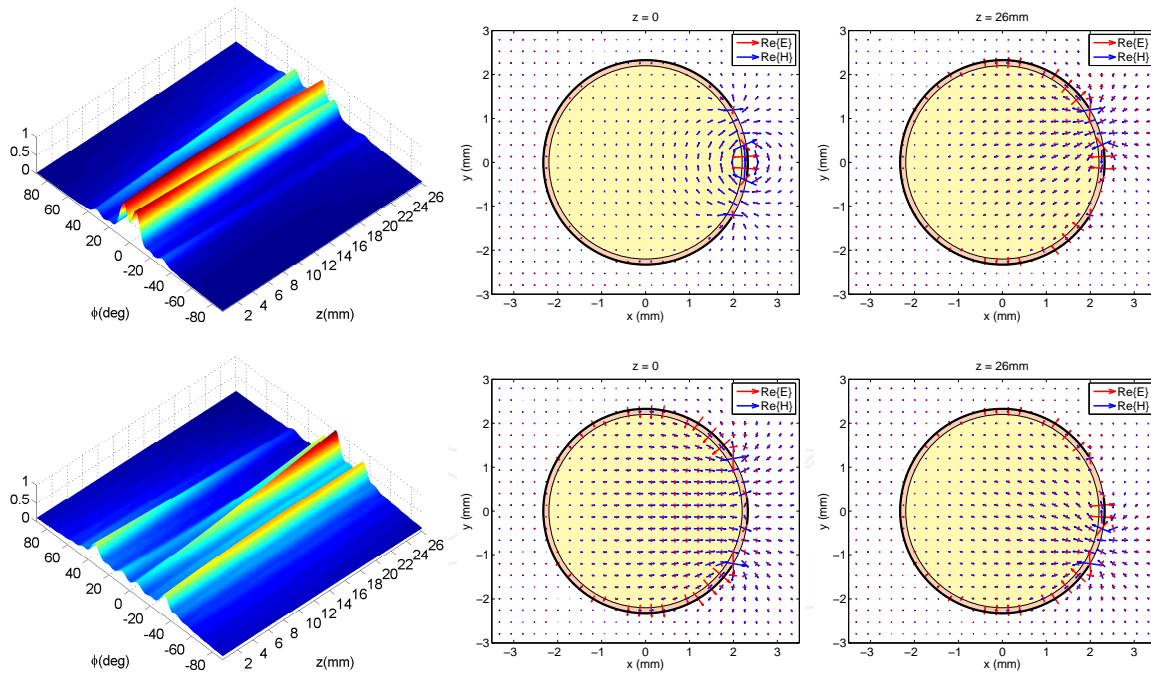


**Figure 17.** Power density and transversal field distribution in the CFCL section for even- (upper row) and odd-mode (bottom row) excitation calculated at $f_0 = 8.2$ GHz

Furthermore, the distributions of the electric and magnetic fields in the input ($z = 0$) and output ports ($z = 26$ mm) of FCL junction providing $45°$ Faraday rotation angle have been calculated. In the analysis, the even- and odd-mode excitations of the junction were assumed. The obtained results confirm the nonreciprocal behavior of the designed CFCL junction.

For the CFCL junction with the ferrite section of length $L = 26$ mm, the scattering parameters were calculated in a function of frequency and presented in Fig. 18.
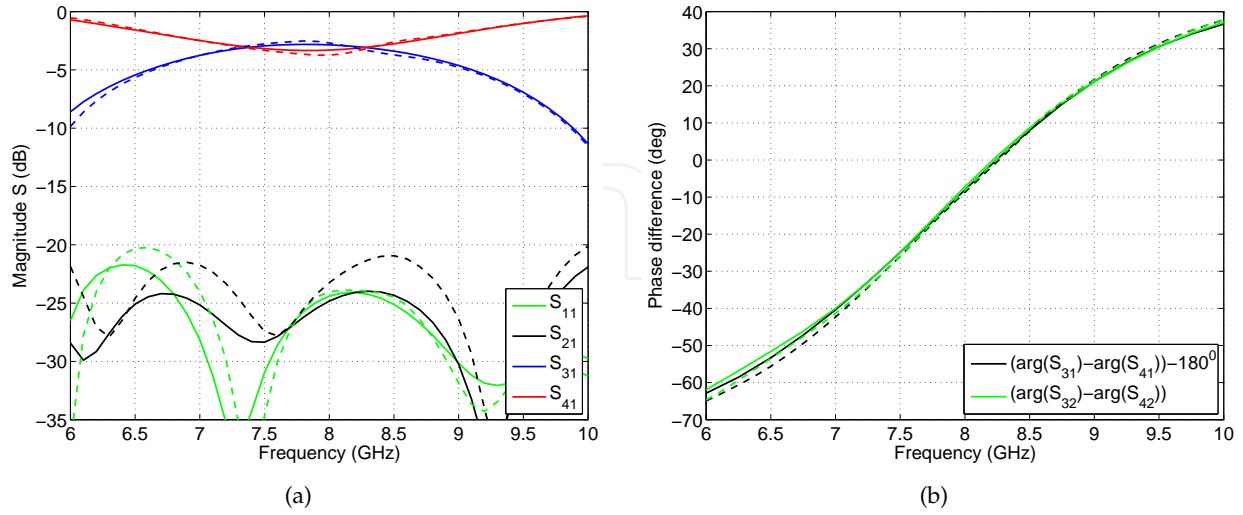


**Figure 18.** Frequency-dependent scattering parameters of CFCL junction for $L = 26$ mm: (a) magnitude and (b) phase difference (solid line, our method; dashed line, HFSS)

From the obtained results, it can be seen that the equal power division defined by $S_{31} = S_{41} = -3 \pm 0.5$ dB is obtained in the frequency range from 7 to 8.6 GHz (see Fig. 18(a)). In this frequency range, the phase difference between the signals in ports (3) and (4) for ports (1) or (2) excitation varies in the range from $-40°$ to $10°$ (see Fig. 18(b)). In addition, it can be seen that the optimal amplitude and phase conditions required for $45°$ Faraday rotation are fulfilled at the frequency $f_0 = 8.25$ GHz. The result of the proposed approach is compared with those obtained from commercial software HFSS, and a good agreement can be observed.

## 4. Nonreciprocal devices

In this section, the results of investigation of nonreciprocal devices made in both the planar and conformal line technology are presented. Section 4.1 presents the results of the three-port circulator realized in slotline technology. Section 4.2 presents the results of a double isolator realized in microstrip coupled lines technology. In Section 4.3, the results of the four-port circulator realized utilizing cylindrical ferrite coupled line section are discussed.

### 4.1. Three-port circulator utilizing ferrite coupled slotline junction

The first investigated circuit is three-port circulator realized in coupled slotline technology, which is shown in Fig 19(a).

The device is realized as a cascade connection of a T-junction, ferrite coupled slotline (FCSL) junction, and the output section being the transformer from the coupled slotlines to the microstrip lines. The cross section of the FCSL junction is shown in Fig. 19(b). The FCSL junction is a four-layer structure, where the coupled slotlines are realized on a thin laminate situated above the ferrite material. The T-junction and the output section have the same cross section as ferrite section, although instead of ferrite, a dielectric material with relative
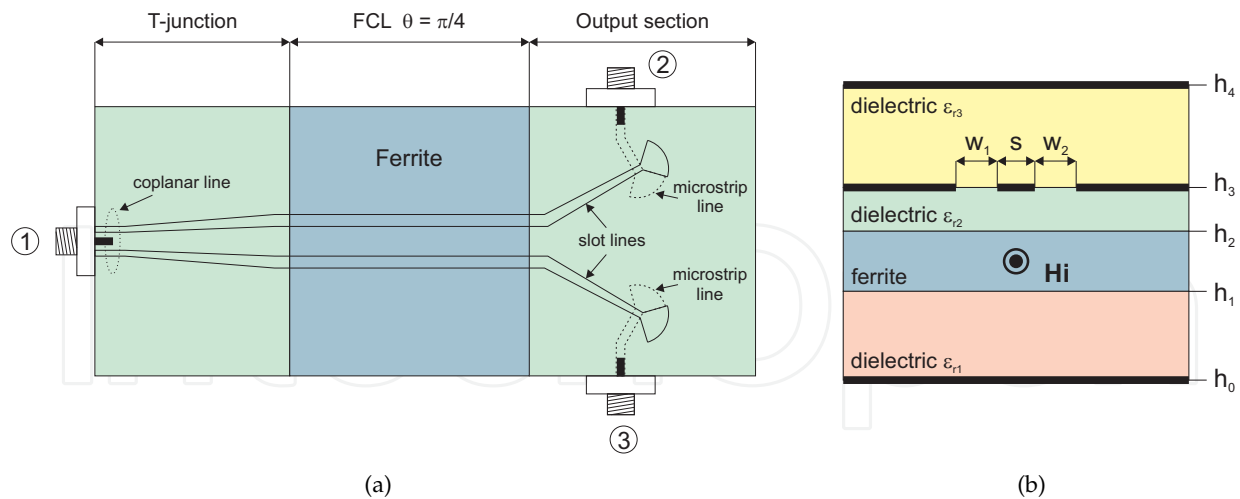
**Figure 19.** FCSL circulator: (a) schematic view of the device and (b) cross section of FCSL junction

permittivity $\varepsilon_r = 9.6$ is used. T-junction is realized as a transformer from coplanar line into coupled slotlines. Due to the fact that the coplanar line is fed from the coaxial connector, the junction provides even excitation of FCSL section. On the other hand, the odd mode, which is transmitted from the ferrite section, is totally reflected in the plane of the coaxial connector. The output structure allows for the transmission of the signal from the specific slot of ferrite junction to the corresponding output microstrip port, while the remaining ports of the circulator are isolated.

In order to determine the scattering parameters of the circulator shown in Fig. 19(a), the scattering matrices of the ferrite junction, T-junction, and output section were first calculated. The scattering parameters of the FCSL junction were simulated with the use of our own software based on the methods described in section 2. The feeding circuits (T-junction and output section) were designed with the use of commercial software. The circulator scattering parameters were obtained by cascade connection of the calculated scattering matrices of individual sections. The simulated frequency characteristics of the scattering parameters are shown in Fig 20.

From the obtained results, it can be seen that the investigated configuration has return losses and isolation better than 10 dB over a wide frequency range from 13 to 20.5 GHz. In the considered frequency band, the average transmission losses are about 1 dB in the case of a single pass of the signal through the ferrite section and about 2 dB in the case of double pass of the signal through the ferrite section. In the analysis, the material losses were not taken into consideration, and the resulting level of losses is due to return losses and the lack of a perfect isolation between the ports of circulator.

A photograph of the manufactured prototype of the circulator is shown in Fig. 21. The measured characteristics of its scattering parameters are depicted in Fig. 22.

Measurements were performed in the frequency range from 10 to 21 GHz. The results show that the investigated device operates in a wide frequency band. In the frequency range from 12 to 19 GHz, the average transmission losses are about 2.5 dB, and the level of isolation and return losses is about 10 dB for a single pass of the signal through the ferrite
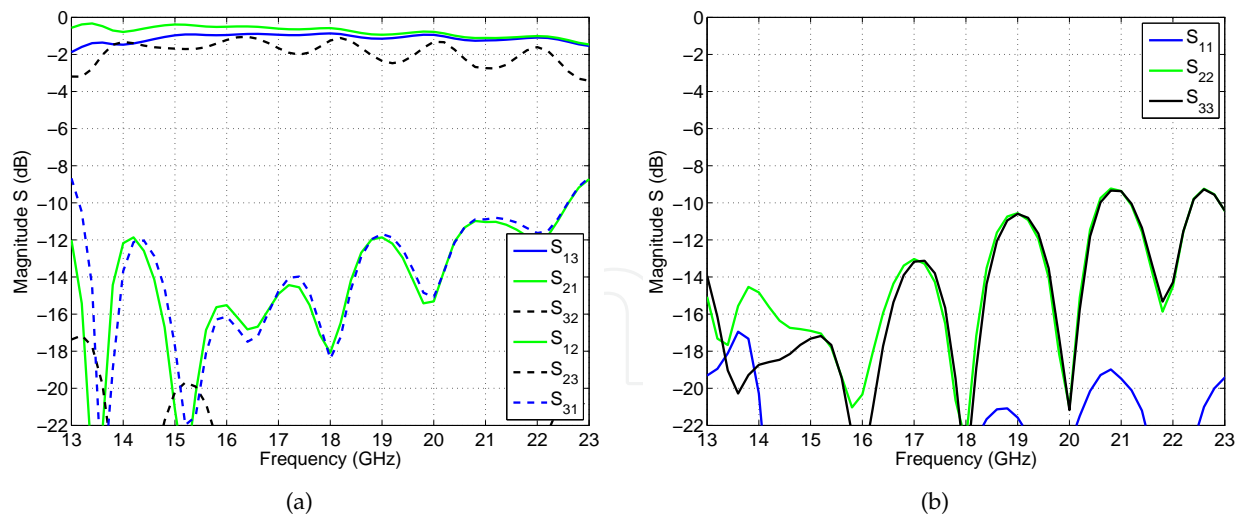
**Figure 20.** Simulated scattering parameters of FCSL circulator: (a) transmission with isolation and (b) reflection
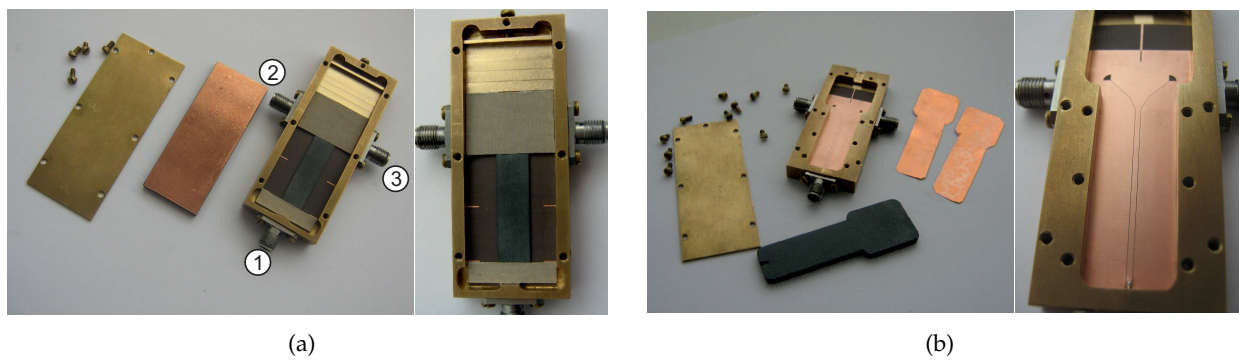


**Figure 21.** Photograph of the fabricated FCSL circulator: (a) top view and (b) bottom view

section. The best isolation is observed in the frequency range from 12 to 15 GHz and is better than 16 dB. In the case of a double pass of the signal through the ferrite section, the transmission losses are two times higher and are about 5.5 dB in the frequency range from 12 to 19 GHz. The isolation is better than 14 dB in the entire frequency range. In the measured transmission characteristics, small periodically repeating resonances occur, which result from the inaccuracies in the manufacturing process.

## 4.2. Double isolator utilizing microstrip coupled line section

Another investigated configuration is a double isolator shown in Fig. 23. This arrangement is composed of two interconnected and magnetized in the same direction three-port circulators (see Fig. 2(c)), in which the appropriate ports are terminated by matched loads. The advantage of this configuration is the ability to achieve high isolation. Unfortunately, due to the fact that the device uses two ferrite sections, the losses in the system are twice as high as in the case of isolator with a single section of FCL.
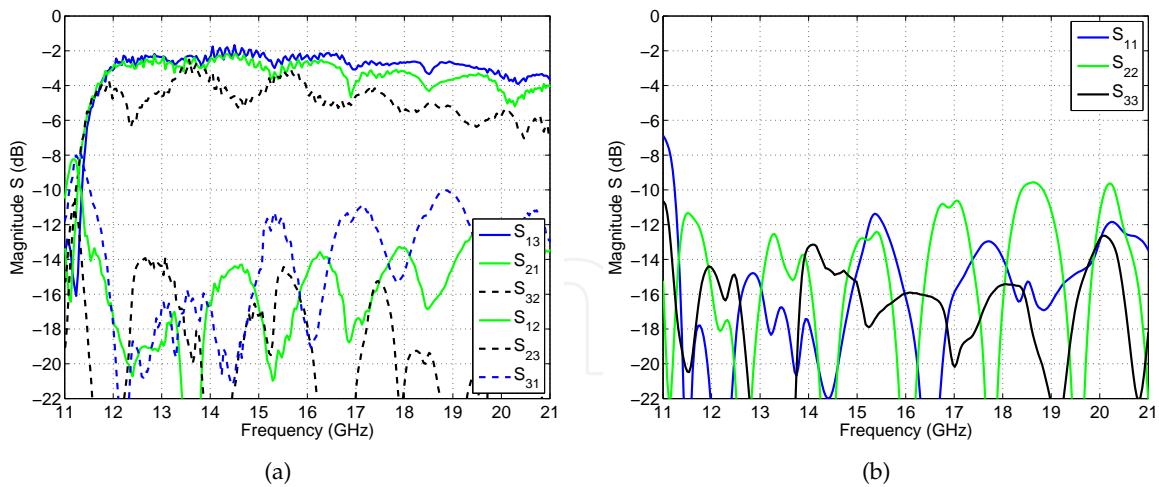
**Figure 22.** Measured scattering parameters of FCSL circulator: (a) transmission with isolation and (b) reflection
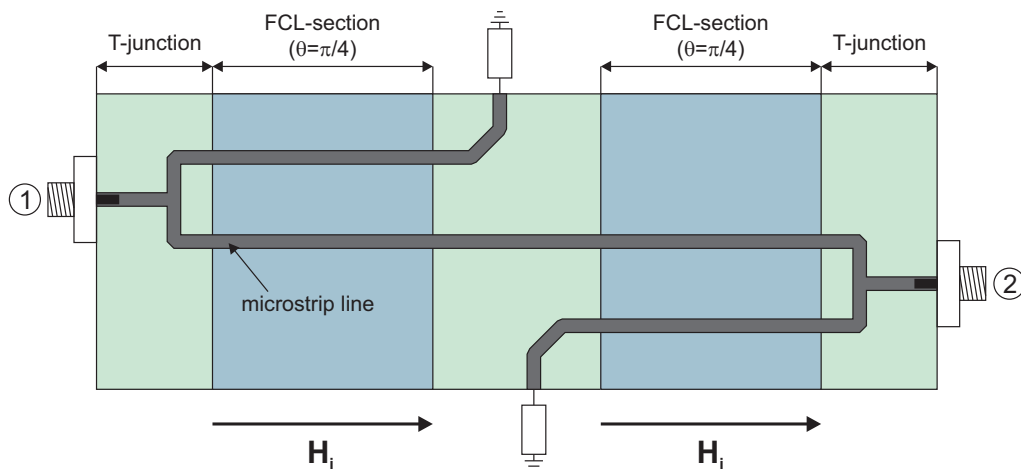


**Figure 23.** Double isolator utilizing microstrip ferrite coupled line junction

Utilizing own software, as well as commercial simulator, the double isolator utilizing ferrite junction from Fig. 8 was designed. The simulation results are shown in Fig. 24.

From the obtained results, it can be seen that in the frequency range from 10 to 16 GHz, the isolation is better than 20 dB with return losses better than 10 dB.

The designed structure was manufactured. A photograph of the prototype is shown in Fig. 25. To obtain the double isolator, ports (3) and (4) of the structure were terminated with the matched SMA connectors. The obtained experimental results are presented in Fig. 26.

It can be seen that the device works in the frequency band from 9 to 16 GHz. In the given frequency range the isolation and the average return losses are better than 15 dB. Furthermore, the average transmission losses are 3.5 dB and they change from 3 dB at 9 GHz to 4 dB at 16 GHz. Based on these results, it can be estimated, that the losses for a single pass of the signal through the investigated microstrip ferrite section are about 1.8 dB. The losses are lower by about 1.5 dB in comparison to the results published for a single section configuration in [4].
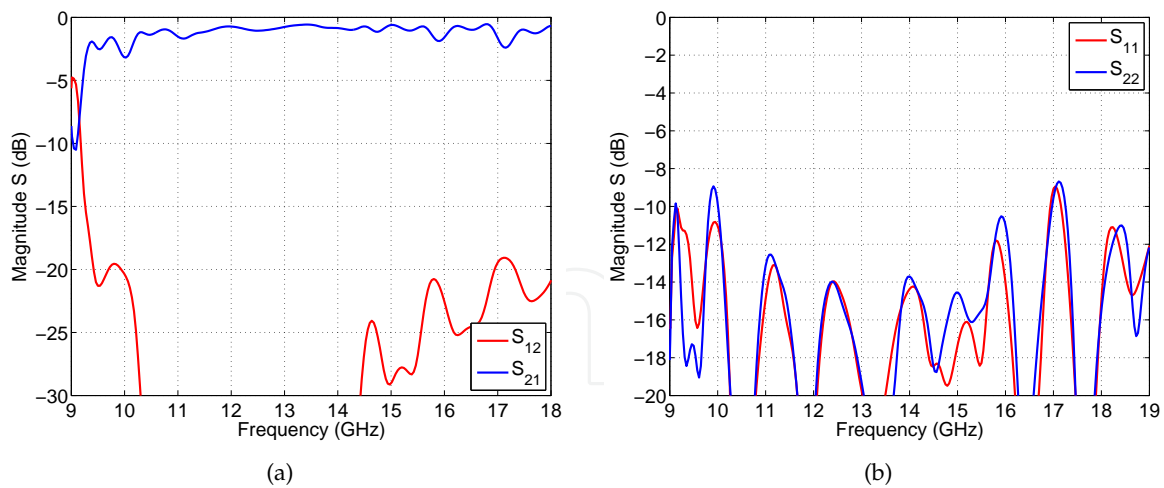
**Figure 24.** Simulated scattering parameters of double MFCL isolator: (a) transmission with isolation and (b) reflection
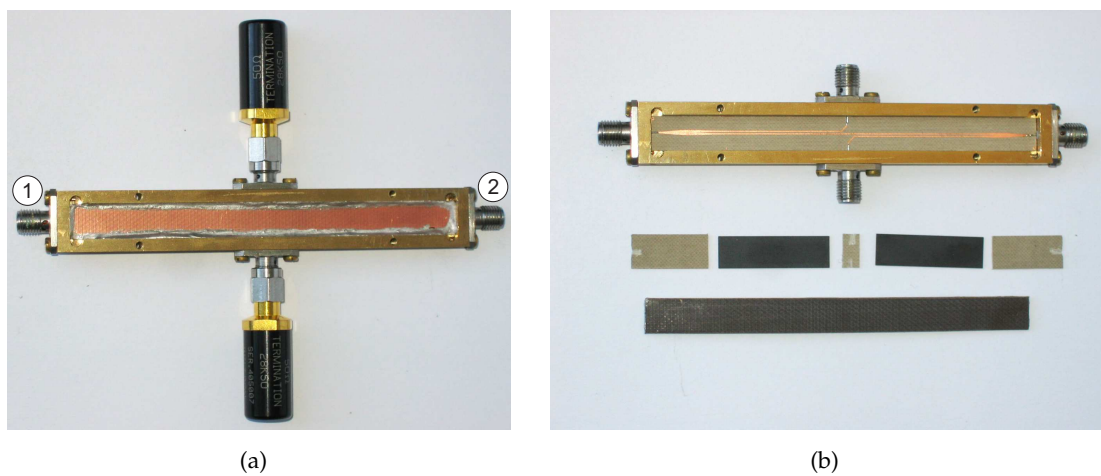


**Figure 25.** Photograph of the manufactured double MFCL isolator

## 4.3. Four-port circulator utilizing cylindrical ferrite coupled line junction

The last investigated device is a four-port circulator shown in Fig. 27. The advantage of this circulator is that the signal transmission in the circulation direction requires only one pass through the ferrite coupled line section. As a result, this allows for reduction of losses in the device in comparison to the alternative configuration of the four-port circulator realized with the use of double ferrite coupled line section.

The investigated device is realized as a cascade connection of the magic-T structure, the CFCL junction, and the output section being the transformer from the cylindrical coupled lines to the uncoupled microstrip lines. The magic-T structure (shown in Fig. 28(a) and (b)) allows to excite ferrite section with odd or even mode.

In the case of port (1) excitation, the signal is transmitted directly through the structure ensuring even mode excitation of cylindrical coupled lines. On the other hand, when port (2) is excited, the signal is coupled to slotline, which results in the odd mode signal at ports (3) and (4). Output section, shown in Fig. 28(c), is a multilayer structure, which transforms
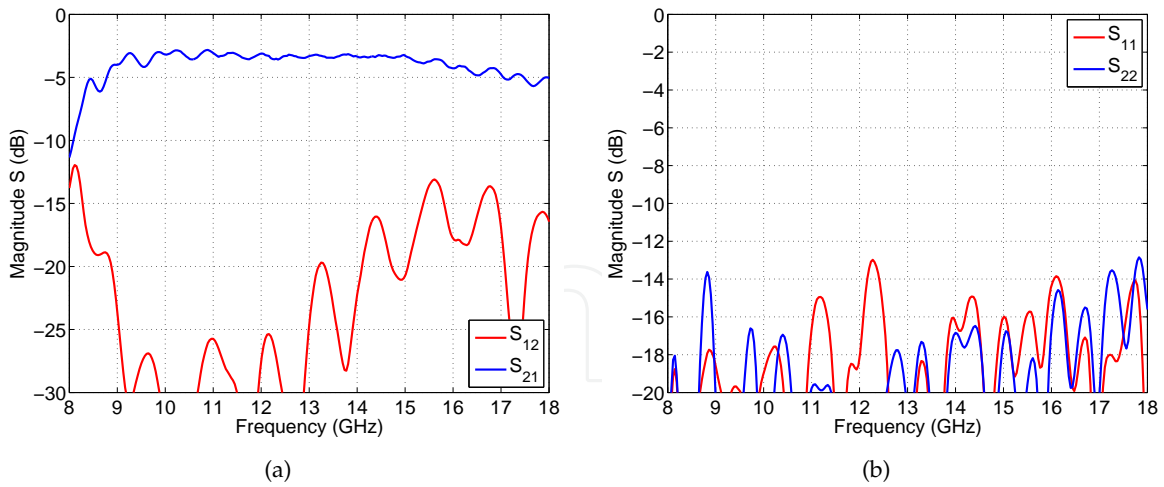
**Figure 26.** Measured scattering parameters of double MFCL isolator: (a) transmission with isolation and (b) reflection
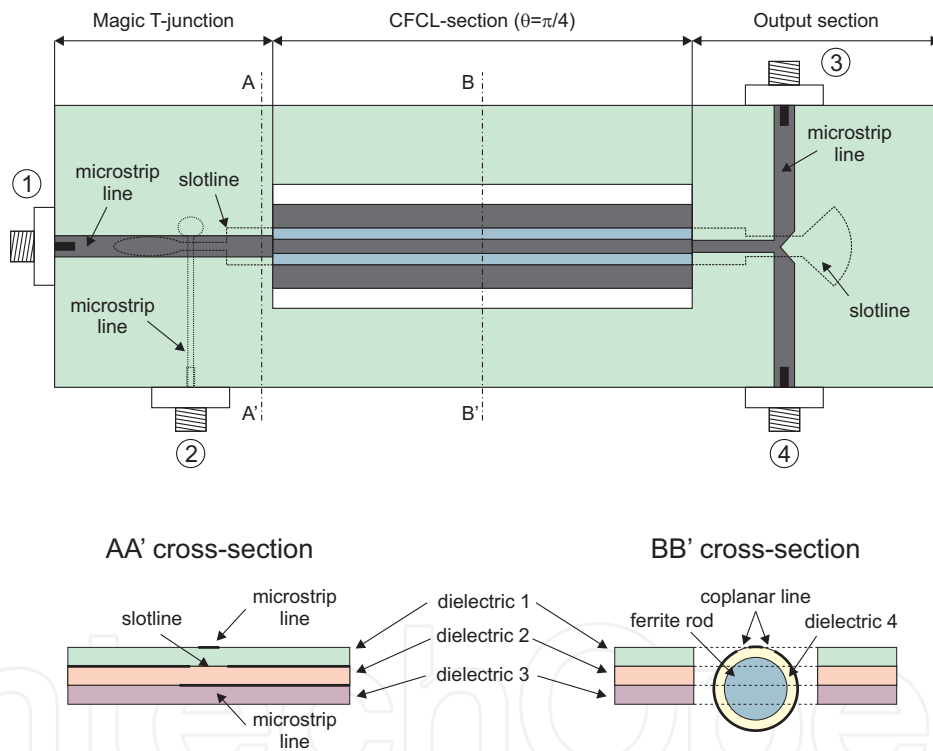


**Figure 27.** Top and bottom view of four-port circulator utilizing cylindrical ferrite coupled line junction

the cylindrical ferrite coupled line to microstrip lines. In the case of port (1) excitation of this section, the signal is transmitted to port (3). Similarly, when port (2) is excited, the signal is transmitted to port (4). For a complete understanding of the operation of the device, the excitation in ports (1) or (2) can be represented as a superposition of the even and odd signals, which are of the same amplitude and phase equal to 0 or 180 °. Then, for even-mode excitation, the signal is divided equally between the output ports. On the other hand, in the case of odd-mode excitation, part of the signal is guided in the bottom slot of the device. Due to the fact that this slotline is shorted with radial stub, the signal is coupled to a microstrip line and divided between the output ports. In order to reduce the isotropic coupling, which
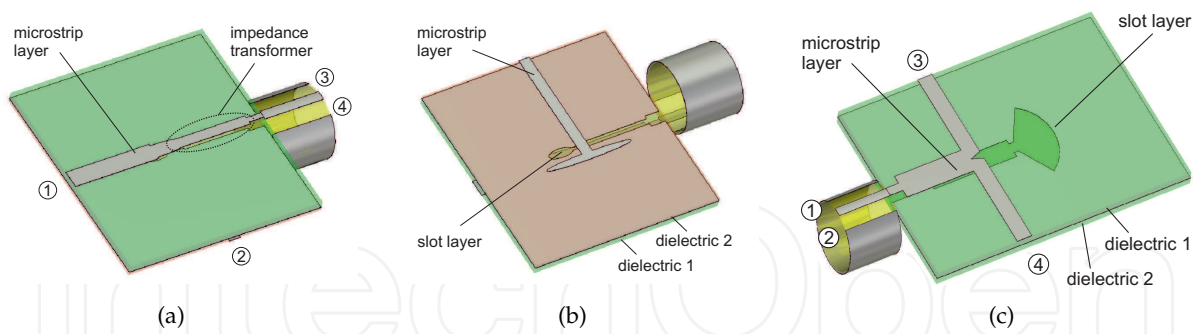
**Figure 28.** Feeding circuits of CFCL circulator: (a) magic T, top view; (b) magic T, bottom view; and (c) output transformer from coupled slotlines to microstrip lines

could deteriorate the isolation of the circulator, an additional dielectric layer is used in the considered structure.

The simulation results of the circulator are presented in Fig. 29. It can be seen that the device operates in the frequency range from 7.6 to 8.6 GHz. In this frequency range, the device isolation and return losses are better than 18 dB. In the analysis, a lossless section was assumed.
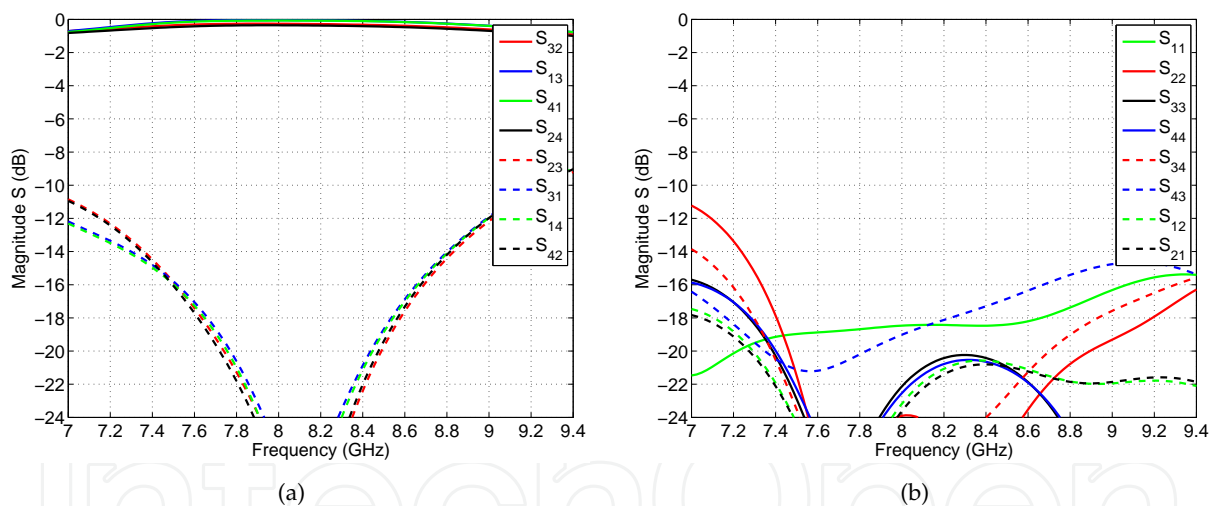


**Figure 29.** Simulated scattering parameters of four-port CFCL circulator: (a) transmission with isolation and (b) reflection coefficients with coupling between neighboring ports

The designed device was manufactured (see the photo in Fig. 30) and measured. The obtained scattering parameters characteristics are shown in Fig. 31.

It can be seen that in the frequency range from 7.6 to 8.6 GHz, the value of transmission from port (1) to (4) and from port (3) to (1) is about $-1.5$ dB, while transmission from port (2) to (3) and port (4) to (2) is about $-3$ dB. The isolation between these ports in the considered frequency range is better than 12 dB. Return losses in ports (2), (3), and (4) are better than 17 dB and in port (1) are better than 8 dB. The isolation between ports (1) and (2) is better than 18 dB and between ports (3) and (4) better than 8 dB. A higher level of return losses
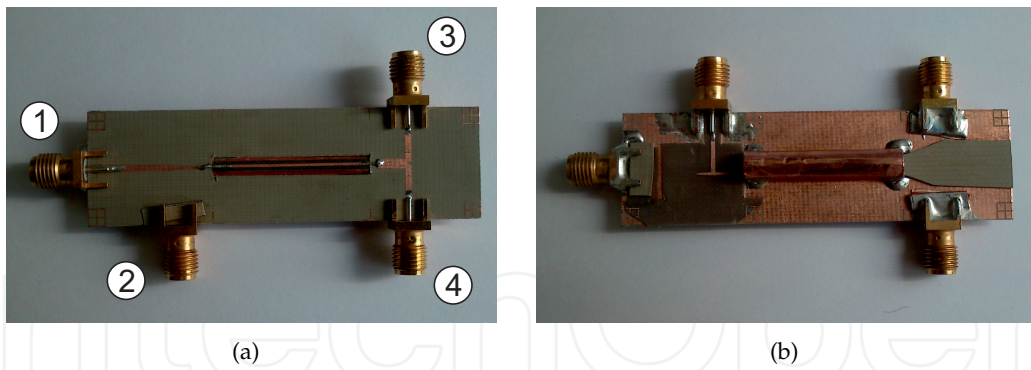
**Figure 30.** Photograph of fabricated four-port CFCL circulator: (a) top view and (b) bottom view
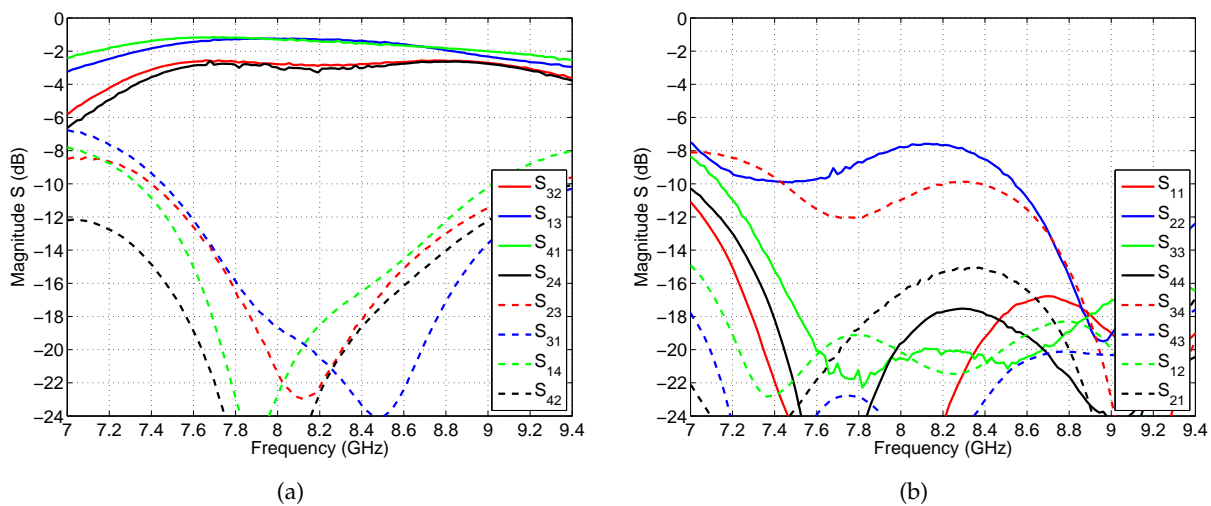


**Figure 31.** Measured scattering parameters of four-port CFCL circulator: (a) transmission with isolation and (b) reflection coefficients and coupling between neighboring ports

and a lower level of isolation with respect to simulated results at port (2) result from the inaccuracy of manufacturing process due to technological limitations. The greatest impact on the deterioration of the device parameters had the positioning of the cylindrical ferrite coupled line section with respect to planar structures. Nevertheless, the obtained results of measurements well agree with the results of simulation.

## 5. Conclusion

In this chapter, the research on nonreciprocal devices utilizing longitudinally magnetized ferrite coupled lines junction is presented. The different configurations of FCL junctions were taken into account, comprising planar lines and conformal guides realized as striplines or slotlines placed on cylinder with circular cross section. The description of developed fast and efficient hybrid methods for the analysis of investigated FCL junctions was presented. The numerical results for planar and conformal FCL junctions were calculated and shown. Finally, the numerical and experimental results concerning nonreciprocal devices utilizing proposed planar and conformal FCL junctions were presented and discussed.

## Acknowledgment

## Author details

Adam Kusiek*, Wojciech Marynowski, Rafal Lech and Jerzy Mazur

*Address all correspondance to: adakus@eti.pg.gda.pl

Gdansk University of Technology, Faculty of Electronics, Telecommunications and Informatics, Poland

## References

[1] Abdalla, M. & Hu, Z. [2009a]. Compact tuneable single and dual mode ferrite left-handed coplanar waveguide coupled line couplers, *Microwaves, Antennas Propagation, IET* **3**(4): 695–702.

[2] Abdalla, M. & Hu, Z. [2009b]. Multi-band functional tunable LH impedance transformer, *Journal of Electromagnetic Waves and Applications* **23**(1): 39–47.

[3] Bahri, R., Abdipour, A. & Moradi, G. [2009]. Analysis and design of new active quasi circulator and circulators, *Progress In Electromagnetics Research PIER* **96**: 377–395.

[4] Cao, M. & Pietig, R. [2005]. Ferrite coupled-line circulator with reduced length, *IEEE Transactions on Microwave Theory and Techniques* **53**(8): 2572–2579.

[5] Cao, M., Pietig, R., Wu, H. C. & Gossink, R. G. [2004]. Perturbation theory approach to the ferrite coupled stripline, *Microwave Symposium Digest, 2004 IEEE MTT-S International* **3**: 1903–1906.

[6] Davis, L. E. & Sillars, D. B. [1986]. Millimetric nonreciprocal coupled slot finline components, *IEEE Transactions on Microwave Theory and Techniques* **34**(7): 804–808.

[7] Fuller, A. J. B. [1986]. *Ferrites at Microwave Frequencies*, Peter Peregrinus Ltd., London UK.

[8] Itoh, T. [1989]. *Numerical Techniques for Microwave and Millimeter-Wave Passive Structures*, John Wiley & Sons, Inc., New York.

[9] Kusiek, A., Marynowski, W. & Mazur, J. [2007]. Investigations of the circulation effects in the structure using ferrite coupled slot-line section, *Microwave and Optical Technology Letters* **49**(3): 692–696.

[10] Kusiek, A., Marynowski, W. & Mazur, J. [2011]. Investigations of cylindrical ferrite coupled line junction using hybrid technique, *Progress In Electromagnetics Research PIER* **120**: 143–164.

[11] Kusiek, A., Marynowski, W. & Mazur, J. [2012]. Investigations of nonreciprocal devices employing cylindrical ferrite coupled line junction, *Journal of Electromagnetic Waves and Applications JEMWA* **26**(13): 1685–1693.

[12] Kusiek, A., Marynowski, W. & Mazur, J. [2013]. Investigations of four-port circulator utilizing cylindrical ferrite coupled line junction, *Progress In Electromagnetics Research PIER* **134**: 379–395.

[13] Marynowski, W., Kusiek, A. & Mazur, J. [2006]. Microstrip ferrite coupled line isolators, *XVI International Microwaves, Radar and Wireless Communications Conference*, Vol. 1, Krakow, Poland, pp. 342–345.

[14] Marynowski, W., Kusiek, A. & Mazur, J. [2008]. Microstrip four-port circulator using a ferrite coupled line section, *AEU - International Journal of Electronics and Communications* **63**(9): 801–808.

[15] Marynowski, W. & Mazur, J. [2008]. Treatment of the three strip coplanar lines on the ferrite, *XVII International Microwaves, Radar and Wireless Communications Conference*, Vol. 1, Wroclaw, Poland, pp. 135–138.

[16] Marynowski, W. & Mazur, J. [2009]. Three-strip ferrite circulator design based on coupled mode method, *2009 International Symposium on Antennas and Propagation (ISAP 2009)*, Bangkok, Thailand, pp. 205–208.

[17] Marynowski, W. & Mazur, J. [2010]. Investigations of the double isolator using three-strip ferrite coupled line, *15th Conference on Microwave Techniques, COMITE 2010*, Brno, Czech Republic, pp. 73–76.

[18] Marynowski, W. & Mazur, J. [2011]. Study of nonreciprocal devices using three-strip ferrite coupled line, *Progress In Electromagnetics Research PIER* **118**: 487–504.

[19] Mazur, J., Mazur, M., Michalski, J. & Sêdek, E. [2002]. Isolator using a ferrite-coupled-lines gyrator, *IEE Proceedings - Microwaves, Antennas and Propagation* **149**(5/6): 291–294.

[20] Mazur, J. & Mrozowski, M. [1989a]. Nonreciprocal operation of structures comprising a section of coupled ferrite lines with longitudinal magnetization direction, *IEEE Transactions on Microwave Theory and Techniques* **37**(6): 1012–1019.

[21] Mazur, J. & Mrozowski, M. [1989b]. On the mode coupling in longitudinally magnetized waveguiding structures, *IEEE Transactions on Microwave Theory and Techniques* **37**(1): 159–164.

[22] Mazur, J., Solecka, M., Mazur, M., Poltorak, R. & Sedek, E. [2005]. Design and measurement of gyrator and isolator using ferrite coupled microstrip lines, *IEE Proceedings - Microwaves, Antennas and Propagation* **152**(1): 43–46.

[23] Mazur, J., Solecka, M., Poltorak, R. & Mazur, M. [2004]. Theoretical and experimental treatment of a microstrip coupled ferrite line circulator, *IEE Proceedings - Microwaves, Antennas and Propagation* **151**(6): 477–480.

[24] Queck, C. K. & Davis, L. E. [2002]. Microstrip and stripline ferrite-coupled-lines (FCL) circulators, *IEEE Transactions on Microwave Theory and Techniques* **50**(12): 2910–2917.

[25] Sajin, G., Simion, S., Craciunoiu, F., Muller, A. & Bunea, A. [2010]. CRLH CPW antenna on magnetically biased ferrite substrate, *Journal of Electromagnetic Waves and Applications* **24**(5–6): 803–814.

[26] Schmidt, L. & Itoh, T. [1980]. Spectral domain analysis of dominant and higher order modes in fin-lines, *IEEE Transactions on Microwave Theory and Techniques* **28**(9): 981–985.

[27] Yang, L.-Y. & Xie, K. [2011]. Design and measurement of nonuniform ferrite coupled line circulator, *Journal of Electromagnetic Waves and Applications* **25**(1): 131–145.

[28] Zahwe, O., Samad, B. A., Sauviac, B., Chatelon, J., Mignon, M. B., Rousseau, J., Berre, M. L. & Givord, D. [2010]. Yig thin film used to miniaturize a coplanar junction circulator, *Journal of Electromagnetic Waves and Applications* **24**(1): 25–32.